# Dioxygen Adducts of Lacunar Cobalt(II) Cyclidene Complexes

**Daryle H. Busch,*,† Patricia J. Jackson,‡ Masaaki Kojima,‡ Piotr Chmielewski,†
Naohide Matsumoto,‡ James C. Stevens,‡ Wei Wu,† Dennis Nosco,‡ Norman Herron,‡ Naidong Ye,†
P. Richard Warburton,† Mohamad Masarwa,† Neil A. Stephenson,† Gary Christoph,‡ and
Nathaniel W. Alcock§**

Departments of Chemistry, The Ohio State University, Columbus, Ohio 43210, University of Kansas,
Lawrence, Kansas 66045, and The University of Warwick, Coventry CV4 7AL, U.K.

The factors controlling the reversible dioxygen binding in lacunar cobalt(II) cyclidene complexes (Figure 1) have been examined. Extensive structural variations reveal that the dioxygen affinity can be controlled by both steric and electronic means. The dioxygen affinity decreases monotonically with the length of a polymethylene bridging group ($R^1$, Figure 1) from octamethylene to tetramethylene; no binding occurs with the still shorter trimethylene bridge. From the analysis of a large array of experimental data, the effects of the $R^2$ and $R^3$ substituents on dioxygen affinity are found to be mainly electronic; for example, electron-withdrawing groups at the $R^2$ and $R^3$ positions decrease the affinity. The various substituent effects are cumulative, but they are not additive. The X-ray crystal structure of the dioxygen adduct $[Co(MeMeC6[16]cyclidene)(1\text{-}MeIm)(O_2)](PF_6)_2$ provides significant insight into the structural relationships. The space group is *Pnma* with $a = 23.226(2)$ Å, $b = 18.981(2)$ Å, and $c = 10.124(1)$ Å. The Co–O–O bond angle is 121(1)°, and the O–O distance is 1.32(2) Å. The conformation of the ligand in this six-coordinate cobalt complex is different from that of the five-coordinate complex, as expected on the basis of structures in which isothiocyanate occupies the cavity. The structural influence of the coordination of a small molecule within the cyclidene cavity is further explored by examination of the crystal structure of the cobalt(III) complex $[Co(MeMeC8[16]cyclidene)(SCN)_2](PF_6)$. The space group is *P$\bar{1}$* with $a = 12.020(3)$ Å, $b = 12.379(3)$ Å, $c = 14.159(4)$ Å, $\alpha = 111.73(2)°$, $\beta = 99.49(2)°$, and $\gamma = 94.57°$. Again, a predicted conformational change accompanies occupation of the lacuna. For a series of complexes having $R^1 = (CH_2)_n$, $R^2 = CH_3$, and various $R^3$ substituents, the dioxygen complexes have been examined by ESR experiments and simulations. From these, the dependence of the Co–O–O bond angles upon the ligand substituents has been evaluated.

## Introduction

Over the last few years the dramatic progress in the chemisty of synthetic dioxygen carriers has been discussed in a number of reviews.[1] A complex with a high and controllable dioxygen affinity and with good stability toward autoxidation and other degradative reactions would find ready application in dioxygen purification and enrichment, chemical sensors, fuels cells, and perhaps even synthetic blood.[2] Comparisons of a number of physical properties of end-on-bound dioxygen adducts with cobalt and iron dioxygen carriers are consistent with the bonding process involving at least partial charge transfer. Reversible dioxygen binding therefore requires a delicate balance in the electronic properties of the metal center, usually cobalt(II) or iron(II). If the metal redox potential (M(III/II)) is too positive, dioxygen binding will not occur; however, a redox potential that is too negative will result in irreversible oxidation of the metal center. Furthermore, all known dioxygen carriers in solution, including hemoglobin, are found to undergo autoxidation, i.e, irreversible oxidation in the
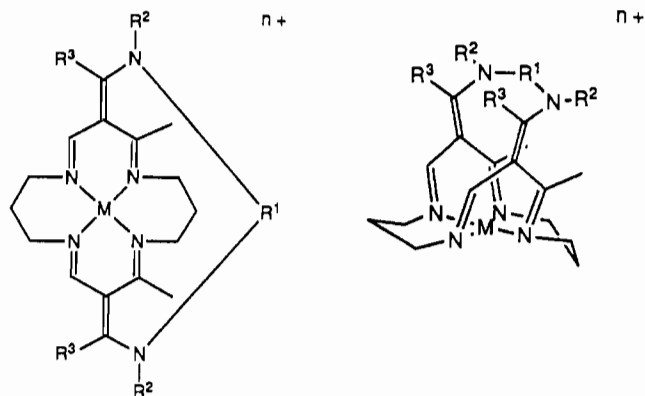


**Figure 1.** General structure for the lacunar cyclidenes: (a, left) flat projection; (b, right) 3-dimensional representation.

presence of dioxygen.[3] The autoxidation of dioxygen carriers was the subject of a recent review.[4] The rate of autoxidation is strongly dependent upon the ligand substituents and experimental conditions, and considerable effort has been made to design ligands which impart oxidative stability while maintaining functional reversible dioxygen binding. In order to achieve a goal of such complexity, detailed knowledge of the factors which affect dioxygen binding is required, and the cobalt(II) and iron(II)

(1) (a) Traylor, T. G., Traylor, P. S. *Annu. Rev. Biophys. Bioeng.* **1982**, *11*, 105. (b) Collman, J. P.; Halpert, T. R.; Suslick, K. S. In *Metal Ion Activation of Dioxygen*; Spiro, T. G., Ed.; Wiley & Sons: New York, 1980. (c) Niederhoffer, E. C.; Timmons, J. H.; Martell, A. E. *Chem. Rev.* **1984**, *84*, 137. (d) Smith, T. D.; Pilbrow, J. T. *Coord. Chem. Rev.* **1981**, *39*, 295. (e) Jones, R. D.; Summerville, D. A.; Basolo, F. *Chem. Rev.* **1979**, *79*, 139. (f) McLendon, G.; Martell, A. E. *Coord. Chem. Rev.* **1976**, *19*, 1. (g) Vaska, L. *Acc. Chem. Res.* **1976**, *9*, 175. (h) Basolo, F.; Hoffman, B. M.; Ibers, J. *Acc. Chem. Res.* **1975**, *8*, 384.
(2) (a) Geyer, R. P. In *Erythrocyte Structure & Function*; Brewer, G. L., Ed.; Alan R. Liss, Inc.: New York, 1974. (b) Busch, D. H. In *Oxygen Complexes and Oxygen Activation by Transition Metals*; Martell, A. E., Sawyer, D. T., Eds.; Plenum Press: New York, 1988.

(3) (a) Eder, H. A.; Finch, C.; McKee, R. W. *J. Clin. Invest.* **1949**, *28*, 265. (b) Dickerson, L. D.; Sauer-Masarwa, A.; Herron, N.; Fendrick, C. M.; Busch, D. H. *J. Am. Chem. Soc.* **1993**, *115*, 3623. (c) George, P.; Stratmann, C. J. *Biochem. J.* **1952**, *51*, 103. (d) George, P.; Stratmann, C. J. *Biochem. J.* **1952**, *51*, 418. (e) George, P.; Stratmann, C. J. *Biochem. J.* **1954**, *57*, 568. (f) Wallace, W. J.; Houtchens, R. A.; Maxwell, J. C. *J. Biol. Chem.* **1982**, *257*, 4966. (g) Satoh, Y.; Shikamma, K. *J. Biol. Chem.* **1981**, *256*, 10272.
(4) Warburton, P. R.; Busch, D. H. *Perspect. Bioinorg. Chem.* **1993**, *2*, 1.

cyclidene complexes have provided an important contribution to this goal. The cyclidene complexes have the general structure shown in Figure 1. Since in this work the macrocyclic skeleton remains constant and only the ligand substituents are varied, the cyclidene complexes may be conveniently denoted in terms of those substituents, as $[M(R^3R^2R^1)]^{n+}$, where M is either Ni(II), Co(II), or Fe(II) and the substituents are as defined in Figure 1. When $R^1$ is a polymethylene chain, it is simplified as C$n$, where $n$ is the number of methylene groups in the chain. Since many components of the ligand structures are readily varied with little change in the synthetic procedures, the cyclidene complexes are well suited for systematic investigation of how ligand parameters affect dioxygen binding.

Preliminary reports on these typical cobalt cyclidene dioxygen carriers[5] and reports on more extreme structural variants[6] have revealed that the dioxygen affinity and resistance to autoxidation of cyclidene complexes depend greatly upon the ligand substituents. Definitive reports recently appeared on the autoxidation processes,[3b,7] and the details of the relationships between dioxygen affinity and substitutents are presented here. For complexes with $R^3 = R^2 = $ Me and $R^1 = $ C$n$ (a polyethylene chain containing $n$ carbon atoms), the dioxygen affinity varies systematically by more than 4 orders of magnitude on varying $n$ from 4 to 8, and that variation parallels a corresponding increase in the width of the cavity of the lacunar complex.[8] Earlier structural and molecular modeling studies have found that the hexamethylene-bridged complex exhibits two low-energy conformations and that one occurs when the cavity is empty and the other when a small ligand is in the cavity.[9] Further, the modeling studies predict that the heptamethylene and octamethylene complexes will also participate in this dual-conformation behavior.[9a] This paper continues these detailed studies by focusing on the dioxygen binding and on the nature of the bound dioxygen and how these features are affected by variations in ligand substituents.

## Experimental Section

**Synthetic Procedures.** **(2,3,11,12,14,20-Hexamethyl-3,11,15,19,22,-26-hexaazabicyclo[11.7.7]heptacosa-1,12,14,19,21,26-hexaene-$\kappa^4N$)cobalt(II) Hexafluorophosphate, [Co$^{II}$(MeMeC7)](PF$_6$)$_2$.** The synthesis

of a related series of cobalt(II) complexes of the form [Co(MeMeC$n$[16]-cyclidene)]$^{2+}$ has been described previously.[10] In this work, the series of complexes for $n = 3$–12 is completed with the synthesis of the complex with $n = 7$. The nickel complex [Ni(MeMeC$n$)]$^{2+}$ was prepared by reaction of the unbridged nickel(II) cyclidene complex [Ni(MeMeH)]$^{2+}$ with the $\alpha,\omega$-ditosylated heptanediol, in strict analogy to the procedures for related complexes.[10] The synthesis of the cobalt(II) complex was achieved, under inert atmosphere, by forming a slurry of cobalt(II) acetate with the ligand salt. The latter was prepared by acidifying an acetonitrile solution of the nickel(II) complex with hydrogen chloride gas and isolating the free ligand salt by addition of an aqueous solution of ammonium hexafluorophosphate.

**(Dioxygen)(2,3,10,11,13,19-hexamethyl-3,10,14,18,21,25-hexaazabicyclo[10.7.7]hexacosa-1,11,13,18,20,25-hexaene-$N_4$)(1-methylimidazole)cobalt(II) Hexafluorophosphate, [Co(MeMeC6)(O$_2$)(1-MeIm)](PF$_6$)$_2$.** This crystalline cobalt(II) dioxygen adduct was prepared from a solution of 0.50 g of [Co(MeMeC6)](PF$_6$)$_2$ (0.63 mmol) dissolved in 10 mL of 1-methylimidazole. Water was added dropwise until the complex began to precipitate (about 10 mL). The mixture was heated to redissolve the solid and then quickly removed from the drybox. Pure dioxygen was blown over the solution for 1 min as the solution turned very dark red. The flask was then placed in a freezer for 2 days, during which time large black crystals formed. The crystals were isolated by pouring off the mother liquid and rinsing with cold ether. The crystals were stable in the freezer for several months, but at room temperature they crumbled in a day or so. For X-ray crystal structure determination, a single crystal was mounted on a glass fiber with epoxy and quickly coated with epoxy to prevent loss of dioxygen.

**Bis(isothiocyanato)(2,3,12,13,15,21-hexamethyl-3,12,16,20,23,27-hexaazabicyclo[12.7.7]octacosa-1,13,15,20,22,27-hexaene-$N_4$)cobalt(III) Hexafluorophosphate, [Co(MeMeC8)(NCS)$_2$](PF$_6$).** Cream-white H$_n$MeMeC8$^{n+}$ ligand salt (0.5344 g) was dissolved in 15 mL of MeOH and 25 mL of MeCN in a 250-mL round-bottomed flask, which was then sealed with a septum. The solution was purged with nitrogen for 15 min using two needles; the inlet was immersed in the solution, and the outlet was near the neck. Co(OAc)$_2\cdot$4H$_2$O (0.1469 g) and NaOAc (0.0484 g) were dissolved in 50 mL of MeOH. After 15 min of nitrogen purging, this liquid was transferred to the flask containing the ligand salt, without exposure to air, by way of a needle. The color of the solution turned orange immediately. NaSCN (0.4783 g, 10-fold excess) was dissolved in 7 mL of water. After this solution was deoxygenated for 15 min, it was also delivered to the cobalt/ligand solution by needle, and the dark red products formed instantaneously. The last reagent, 0.3235 g of ammonium cerium(IV) nitrate, (NH$_4$)$_2$Ce(NO$_3$)$_6$, in 50 mL of MeOH, was purged with nitrogen for 15 min and was added to the red solution via needle. The resulting red solution was left stirring under nitrogen overnight.

All of the solvent was removed by a rotary evaporator, and the oily green residue was redissolved in the minimum amount of MeCN. The red solution was loaded onto a neutral alumina column. Acetonitrile was used as the eluent. The first red-brown band was collected, and its volume was reduced on a rotary evaporator. NH$_4$PF$_6$ (290 mg) in methanol was mixed with the above product to ensure the formation of the hexafluorophosphate salt. The solution was put in a rotary evaporator, and methanol was incrementally added, so as to gradually increase the proportion of methanol in the solvent. After a red-brown solid started to form, the solution was placed in a refrigerator overnight. The following day, the red-brown crystals were collected by suction filtration, washed with ethanol, and dried in vacuo. Yield: 0.1154 g (25%).

**Physical Methods.** Solvents were purified according to published methods.[11] All inert-atmosphere manipulations were performed in a nitrogen-filled Vacuum Atmospheres Corp. (VAC) glovebox, equipped with a gas circulation and dioxygen removal system consisting of either a VAC MO40-1 or an HE-493 dry train. UV–visible spectrophotometric studies were conducted using a 1-cm gastight quartz cell, fitted with a gas inlet and a bubbling tube. Spectra were recorded on either a Varian 2300 spectrophotometer or a Hewlett Packard 8452 diode array spectrophotometer, with a 9000 (300) Hewlett Packard Chem Station. The Varian spectrophotometer was connected to an IBM personal

(5) (a) Stevens, J. C.; Busch, D. H. *J. Am. Chem. Soc.* **1980**, *102*, 3285. (b) Busch, D. H.; Stephenson, N. A. In *Inclusion Compounds*; Atwood, J., Davies, E., MacNichol, Eds.; Inorganic & Physical Aspects of Inclusion, Vol. 5; Oxford University Press: Oxford, U.K., 1991.

(6) (a) Herron, N.; Busch, D. H. *J. Am. Chem. Soc.* **1981**, *103*, 1236. (b) Herron, N.; Chavan, M. Y.; Busch, D. H. *J. Chem. Soc., Dalton Trans.* **1984**, 1491. (c) Busch, D. H. *Trasfus. Sangue* **1988**, *33*, 57. (d) Herron, N.; Schammel, W. P.; Jackels, S. J.; Grzybowski, J. J.; Zimmer, L. L.; Busch, D. H. *Inorg. Chem.*, **1983**, *22*, 1433. (e) Cameron, J. H.; Kojima, M.; Korybut-Daszkiewicz, B.; Coltrain, B. K.; Meade, T. J.; Alcock, N. W.; Busch, D. H. *Inorg. Chem.* **1987**, *26*, 427. (f) Hoshino, N.; Jircitano, A.; Busch, D. H. *Inorg. Chem.* **1988**, *27*, 2292. (g) Thomas, R.; Fendrick, C. M.; Lin, W.-K.; Glogowski, M. W.; Chavan, M. Y.; Alcock, N. W.; Busch, D. H. *Inorg. Chem.* **1988**, *27*, 2534. (h) Tweedy, H. E.; Alcock, N. W.; Matsumoto, N.; Padolik, P. A.; Stephenson, N. A.; Busch, D. H. *Inorg. Chem.* **1990**, *29*, 616. (i) Padolik, P. A.; Jircitano, A. J.; Alcock, N. W.; Busch, D. H. *Inorg. Chem.* **1991**, *30*, 2713. (j) Chen, J.; Ye, N.; Alcock, N. W.; Busch, D. H. Inorg. Chem. **1993**, *32*, 904.

(7) (a) Masarwa, M.; Warburton, P. R.; Evans, W. E.; Busch, D. H. *Inorg. Chem.* **1993**, *32*, 3826. (b) Sauer-Masarwa, A.; Dickerson, L. D.; Herron, N.; Busch, D. H. *Coord. Chem. Rev.* **1993**, *128*, 117. (c) Sauer-Masarwa, A.; Herron, N.; Fendrick, C. M.; Busch, D. H. *Inorg. Chem.* **1993**, *32*, 1086. (d) Herron, N.; Zimmer, L. L.; Grzybowski, J. J.; Olszanski, D. J.; Jackels, S. C.; Callahan, R. W.; Cameron, J. H.; Christoph, G. C.; Busch, D. H. *J. Am. Chem. Soc.* **1983**, *105*, 6585. (e) Herron, N.; Dickerson, L. D.; Busch, D. H. *J. Chem. Soc., Chem. Commun.* **1983**, 884.

(8) The width is defined as either the distance between the pairs of nitrogen atoms in the superstructure or the distance between the carbon atoms to which those nitrogens are attached.

(9) (a) Lin, W.-K.; Alcock, N. W.; Busch, D. H. *J. Am. Chem. Soc.* **1991**, *113*, 7603. (b) Alcock, N. W.; Padolik, P. A.; Pike, G. A.; Kojima, M.; Cairns, C. J.; Busch, D. H. *Inorg. Chem.* **1990**, *29*, 2599. (c) Alcock, N. W.; Lin, W.-K.; Cairns, C.; Pike, G. A.; Busch, D. H. *J. Am. Chem. Soc.* **1989**, *111*, 6630. (d) Alcock, N. W.; Lin, W.-K.; Jircitano, A.; Mokren, J. D.; Corfield, P. W. R.; Johnson, G.; Novotnak, G.; Cairns, C.; Busch, D. H. *Inorg. Chem.* **1987**, *26*, 440.

(10) (a) Cairns, C. J.; Busch, D. H. *Inorg. Synth.* **1990**, *27*, 261. (b) Chia, P. S. K.; Masarwa, M.; Warburton, P. R.; Wu, W.; Kojima, M.; Nosco, D.; Alcock, N. W.; Busch, D. H. *Inorg. Chem.* **1993**, *32*, 2736.

(11) (a) Perrins, D. D.; Amarego, W. L. F.; Perrins, D. R. *Purification of Laboratory Chemicals*; Pergamon Press: Oxford, U.K., 1980. (b) Schriver, D. F.; Drezdon, M. A. *The Manipulation of Air-Sensitive Compounds*, 2nd ed.; John Wiley & Sons: New York, 1986.
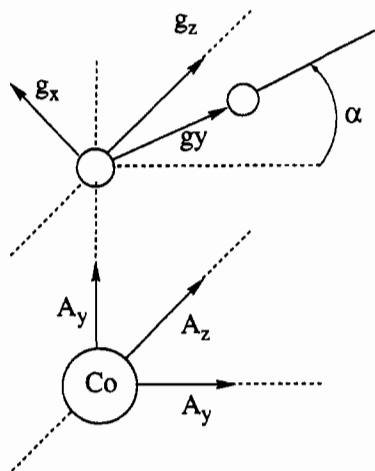
**Figure 2.** Coordinate system for Zeeman and hyperfine terms of the ESR spectra.

**Table 1.** Data Collection and Refinement Details for X-ray Structural Determinations

| complex | [CoL(O₂)(1-MeIm)](PF₆)₂ | [CoL(SCN)₂]PF₆·H₂O |
|---|---|---|
| empirical formula | CoC₃₄H₅₆N₁₀O₂P₂F₁₂ | C₃₀H₄₈N₈S₂CoPF₆·H₂O |
| fw | 985.7 | 788.7 + 18.0 |
| cryst system | orthorhombic | triclinic |
| space group | *Pnma* | *P*1̄ |
| *a*, Å | 23.226(2) | 12.020(3) |
| *b*, Å | 18.981(2) | 12.379(3) |
| *c*, Å | 10.124(1) | 14.159(4) |
| α, deg | | 111.73(2) |
| β, deg | | 99.49(2) |
| γ, deg | | 94.57(2) |
| *V*, Å³ | 4463 | 1907.4(8) |
| *Z* | 4 | 2 |
| density, g/cm³ | 1.47 (expt) | 1.40 (calc) |
| Mo Kα λ, Å | 0.710 69 | 0.710 69 |
| μ(Mo Kα), cm⁻¹ | 5.4 | 6.6 |
| no. of idivid reflns | 5500 | 6761 |
| no. of reflcns with $I/\sigma(I)$ ≥ 2.0 | 1126 | 5011 |
| *R* | 0.126 | 0.070 |
| *S* | | 0.096 |
| *R*�w | 0.138 | 1.72 |
| *T*, K | 290 | 290 |

computer, which controlled the spectrometer and allowed automated data collection. Both instruments incorporated flow-through temperature-regulated cell holders connected to a Neslab or Fisher Scientific constant-temperature circulation system, giving a temperature precision of ±0.2 °C. Dioxygen/nitrogen gas mixtures were produced using Tylan FC-260 mass flow controllers.

Electrochemical experiments were performed within the glovebox, using a single-compartment cell. The working electrode was a 3 mm diameter glassy carbon electrode in Kel-F (Bioanalytical Systems); the secondary electrode was a platinum wire; and a silver wire was used for the reference electrode. Potentials were measured versus ferrocene, which was used as an internal standard. The experiments were undertaken using a Princeton Applied Research (PAR) Model 175 programmer and a PAR Model 173 potentiostat, and the output was directly recorded on paper using a Houston Instruments Model 200 X-Y recorder.

Equilibrium constants for the formation of the 1:1 cobalt–dioxygen adducts were determined by monitoring UV–visible changes as a function of a partial pressure of dioxygen[5a,12] and were fitted, on an IBM Model 80 PS/2 computer, to the Ketelaar equation,[13] using a BASIC program written in this research group.

(12) Stevens, J. C. Ph.D. Thesis, The Ohio State University, 1979.
(13) Ketelaar, J. A. A.; Van de Stolpe, C.; Gouldsmit, A.; Dzcubas, W. *Recl. Trav. Chim. Pays-Bas* **1952**, *71*, 1104.

**Table 2.** Atom Coordinates (×10⁴) for the Dioxygen Adduct [Co(MeMeC6)(1-MeIm)(O₂)](PF₆)₂

| atom | *x* | *y* | *z* |
|---|---|---|---|
| Co | 1535(1) | 2500 | 224(3) |
| P | 3558(2) | 374(3) | −2583(7) |
| F(1) | 3071(7) | 933(7) | −2980(18) |
| F(2) | 3210(7) | 124(8) | −1286(17) |
| F(3) | 4016(10) | −181(14) | −2140(30) |
| F(4) | 3914(7) | 608(8) | −3847(19) |
| F(5) | 3825(7) | 907(11) | −1692(25) |
| F(6) | 3287(13) | −185(10) | −3456(31) |
| O(1) | 1309(6) | 2500 | −1521(14) |
| O(2) | 1694(8) | 2500 | −2484(19) |
| N(1) | 973(5) | 1733(7) | 507(13) |
| N(2) | 2087(8) | 1740(7) | −211(13) |
| N(3) | 1782(8) | 2500 | 2191(18) |
| N(4)ᵃ | 935(20) | 554(24) | −2926(45) |
| N(41)ᵃ | 626(23) | 912(29) | −3276(58) |
| N(5) | 3698(10) | 2500 | 4724(23) |
| C(1) | 228(24) | 2500 | 1590(61) |
| C(2) | 541(9) | 1816(11) | 1636(23) |
| C(3) | 922(9) | 1203(12) | −230(22) |
| C(4) | 389(8) | 703(11) | −141(21) |
| C(5) | 1329(8) | 1018(9) | −1110(18) |
| C(6) | 1981(8) | 1186(9) | −835(17) |
| C(7) | 2697(6) | 1831(8) | 192(16) |
| C(8) | 2929(8) | 2500 | −517(17) |
| C(9)ᵃ | 1241(22) | 472(26) | −1981(50) |
| C(91)ᵃ | 1250(29) | 861(36) | −2330(64) |
| C(10)ᵃ | 1681(26) | 358(31) | −3123(65) |
| C(101)ᵃ | 1691(52) | −42(57) | −2264(104) |
| C(11)ᵃ | 703(25) | 93(30) | −3830(54) |
| C(12)ᵃ | 365(29) | 1251(35) | −2958(71) |
| C(13)ᵃ | −69(16) | 1792(21) | −4571(38) |
| C(131)ᵃ | 516(74) | 1366(92) | −4390(161) |
| C(140)ᵃ | −59(63) | 2125(65) | −4182(152) |
| C(14)ᵃ | −80(26) | 2500 | −3923(66) |
| C(141)ᵃ | 249(46) | 1684(48) | −5651(104) |
| C(15) | 1870(9) | 1925(11) | 2926(21) |
| C(16) | 2067(7) | 2104(8) | 4063(16) |
| C(17)ᵃ | 2199(34) | 1624(37) | 5081(73) |
| C(18) | 3707(23) | 2500 | 6242(55) |
| C(19) | 3752(10) | 1980(13) | 3884(24) |
| C(20) | 3756(9) | 2104(11) | 2695(21) |

ᵃ Occupancy 0.5.

Infrared spectra were obtained using a Perkin-Elmer FTIR Model 1600 spectrophotometer. Samples were examined either as potassium bromide disks or in acetonitrile solution. Fast atom bombardment (FAB) mass spectra were obtained on a VG ZAB HS mass spectrometer equipped with a xenon gun. The FAB experiments were performed either in a matrix composed of a 3:1 mixture of dithiothreitol and dithioerythritol (FAB/MB) or in 3-nitrobenzyl alcohol (FAB/NBA). Elemental analyses were performed at the University of Kansas or by Galbraith Laboratories Inc., Knoxville, TN. ¹³C NMR spectra were obtained on a Varian XL-300 spectrometer operating at 75.43 MHz and a Bruker AM-500 spectrometer operating at 125.76 MHz. ¹H NMR were obtained on the same spectrometers operating at 299.94 MHz and 500.14 MHz, respectively. Signal positions are reported in parts per million (ppm) relative to residual solvent signals. ESR spectra were recorded on a Varian E-112 spectrometer operating in the X-band.

**Simulations of ESR Spectra.** ESR spectra of dioxygen adducts of cobalt cyclidene complexes were examined in a systematic manner, using a model designed to treat these particular ESR spectra and originally described by Smith and Pilbrow.[1d] The g and A tensors were assumed to be noncoincident. In such a model, the coordinate system of A is rotated around the *z* axis by an angle of α, which is common for both g and A coordinate systems, as shown in Figure 2. In the simulation procedure 10 parameters were considered: $g_x$, $g_y$, $g_z$, $A_x$, $A_y$, $A_z$, line widths $\sigma_x$, $\sigma_y$, $\sigma_z$, and α. Spectra were calculated for 30 values of the θ angle (θ varies from 0 to π/2) and 60 values of the φ angle (variation from 0 to π). The orientation-dependent transition probability was calculated according to Aäsa and Vängård.[14] Spectra were fitted by means of the Marquardt method[15] with 150 field points using the difference

(14) Aäsa, R.; Vängård, T. *J. Magn. Reson.* **1972**, *19*, 308.
(15) Marquardt, D. W. *SIAM J.* **1963**, *11*, 431.

**Table 3.** Bond Lengths (Å) and Angles (deg) for the Dioxygen Adduct [Co(MeMeC6)(1-MeIm)(O₂)](PF₆)₂[a]

| | | | |
|---|---|---|---|
| Co–O(1) | 1.844(15) | Co–N(1) | 1.976(13) |
| Co–N(2) | 1.979(13) | Co–N(3) | 2.072(19) |
| P–F(1) | 1.602(15) | P–F(2) | 1.614(18) |
| P–F(3) | 1.563(25) | P–F(4) | 1.586(20) |
| P–F(5) | 1.491(23) | P–F(6) | 1.517(27) |
| O(1)–O(2) | 1.323(24) | N(1)–C(2) | 1.529(26) |
| N(1)–C(3) | 1.259(26) | N(2)–C(6) | 1.252(22) |
| N(2)–C(7) | 1.485(20) | N(3)–C(15) | 1.358(24) |
| N(5)–C(19) | 1.441(29) | N(5)–C(18) | 1.536(61) |
| C(1)–C(2) | 1.489(35) | C(3)–C(4) | 1.563(29) |
| C(3)–C(5) | 1.345(28) | C(5)–C(6) | 1.571(25) |
| C(7)–C(8) | 1.555(18) | C(15)–C(16) | 1.252(27) |
| C(16)–C(17) | 1.409(74) | C(16)–C(16′) | 1.503(31) |
| C(1g)–C(20) (in selected disordered chain) | 1.271(33) | C(20)–C(20′) | 1.502(41) |
| C(5)–C(9) | 1.38(5) | C(9)–C(101) | 1.46(13) |
| C(9)–N(4) | 1.21(7) | N(4)–C(12) | 1.87(8) |
| C(12)–C(131) | 1.51(18) | C(131)–C(13), C(13′)–C(131′) | 1.59(18) |
| C(13)–C(14), C(14)–C(13′) | 1.50(5) | C(131′)–N(41′) | 1.44(18) |
| N(41′)–C(11′) | 1.66(8) | N(41)–C(91′) | 1.74(8) |
| C(91′)–C(5′) | 1.28(7) | O(1)–Co–N(2) | 88.3(5) |
| O(1)–Co–N(1) | 87.2(5) | O(1)–Co–N(3) | 179.6(7) |
| N(1)–Co–N(2) | 85.6(5) | N(2)–Co–N(3) | 92.0(5) |
| N(1)–Co–N(3) | 92.5(5) | N(1)–Co–N(1a) | 94.9(7) |
| O(1)–Co–N(1a) | 87.2(5) | F(1)–P–F(3) | 177.4(12) |
| N(2)–Co–N(1a) | 175.5(6) | F(1)–P–F(4) | 88.8(9) |
| O(1)–Co–N(2a) | 88.3(5) | F(3)–P–F(4) | 93.7(12) |
| N(2)–Co–N(2a) | 93.6(8) | F(2)–P–F(5) | 85.2(11) |
| F(1)–P–F(2) | 92.7(9) | F(4)–P–F(5) | 94.6(11) |
| F(2)–P–F(3) | 84.8(12) | F(2)–P–F(6) | 93.5(13) |
| F(2)–P–F(4) | 178.5(9) | F(4)–P–F(6) | 86.7(13) |
| F(1)–P–F(5) | 89.8(10) | Co–O(1)–O(2) | 120.9(12) |
| F(3)–P–F(5) | 90.0(13) | Co–N(1)–C(3) | 124.4(13) |
| F(1)–P–F(6) | 91.5(12) | Co–N(2)–C(6) | 126.7(12) |
| F(3)–P–F(6) | 88.7(14) | C(6)–N(2)–C(7) | 115.1(14) |
| F(5)–P–F(6) | 178.2(14) | Co–N(3)–C(15a) | 126.5(11) |
| Co–N(1)–C(2) | 117.8(11) | C(18)–N(5)–C(19a) | 126.1(13) |
| C(2)–N(1)–C(3) | 117.7(15) | C(2)–C(1)–C(2a) | 121.3(41) |
| Co–N(2)–C(7) | 118.2(10) | N(1)–C(3)–C(4) | 121.7(18) |
| Co–N(3)–C(15) | 126.5(11) | C(4)–C(3)–C(5) | 116.0(18) |
| C(15)–N(3)–C15a) | 107.0(22) | C(3)–C(5)–C(9) | 121.0(27) |
| C(18)–N(5)–C(19) | 126.1(13) | C(3)–C(5)–C(1′) | 126.6(34) |
| C(19)–N(5)–C(19a) | 106.8(25) | N(2)–C(7)–C(8) | 107.4(13) |
| N(1)–C(2)–C(1) | 112.8(27) | C(15)–C(16)–C(17) | 123.7(33) |
| N(1)–C(3)–C(5) | 122.3(19) | C(17)–C(16)–C(16a) | 130.3(30) |
| C(3)–C(5)–C96) | 120.4(16) | C(19)–C(20)–C(20a) | 108.6(15) |
| C(6)–C(5)–C(9) | 114.2(25) | | |
| C(6)–C(5)–C(91′) | 110.9(32) | | |
| N(2)–C(6)–C(5) | 116.7(15) | | |
| C(7)–C(8)–C(7a) | 109.4(16) | | |
| N(3)–C(15)–C(16) | 110.4(18) | | |
| C(15)–C(16)–C(16a) | 105.8(12) | | |
| N(5)–C(19)–C(20) | 107.7(21) | | |

[a] Primed atoms are related to unprimed atoms by (x, 0.5 – y, z).

between the experimental and simulated spectra in the first derivative of intensity as an optimized function. Simulations were carried out on an IBM PS/2 Model 80 microcomputer. The program used for the simulation was written in Pascal by P.C.

**X-ray Structure Determination for the Dioxygen Adduct [Co-(MeMeC6)(O₂)(1-MeIm)](PF₆)₂.** Data were collected with a Syntex P1̄ four-circle diffractometer. Maximum 2θ was 60°; backgrounds were measured at each end of the scan for 0.5 of the scan time. The crystals were of poor quality and diffracted weakly. Three standard reflections were monitored every 100 reflections and showed slight decay during data collection; the data were rescaled to correct for this. Unit cell dimensions and standard deviations were obtained by a least-squares fit to 15 reflections. A total of 5500 unique reflections were collected, of which only the 1126 with $I/\sigma(I) \geq 2.0$ were used in refinement (corrected for Lorentz and polarization effects but not for absorption). Systematic absences (0kl, k + l ≠ 2n; hk0, h ≠ 2n) indicate either space group *Pnma* with the cation required to lie on a mirror plane or *Pn2₁a* (nonstandard setting of *Pna2₁*) with no constraints. The former was initially selected and is considered to be correct for the reasons discussed below. The Co atom was located from a Patterson synthesis, and light atoms were located from successive Fourier syntheses, apart from the C6 bridge atoms. Peaks in that area appeared on Fourier syntheses, but with very low peak heights, while the largest peak in the central part of the

bridge lay on the mirror plane, inconsistent as part of a chain containing an even number of atoms. Both the coordinated N-methylimidazole and a second uncoordinated molecule lie across the mirror plane. The coordinated molecule has substitutional disorder of the methylated nitrogen and the adjacent carbon atom, and the methyl group occurs in two alternative positions with 50% occupancy. In the free imidazole, the methyl group lies on the mirror plane, so it is only affected by disorder of the nonmethylated nitrogen atom and an adjacent carbon atom. These N/C disordered atoms were given carbon scattering factors. These imidazole groups, the PF₆⁻ group, the bound dioxygen, and the atoms of the cyclidene unit refined satisfactorily in *Pnma*. The H atoms of CH and CH₂ (but not Me) groups were included at calculated positions. Because of the very limited data, anisotropic thermal parameters were used only for Co, P, and F. Initial refinement of the remaining cyclidene atoms and the bridge was more difficult. Their thermal parameters took on very high values while significant peaks remained on difference syntheses. Satisfactory refinement was achieved by using alternative positions for N(4) and C(9)–C(11) and approximating the unique half of the bridge by six atoms; all of these atoms were given 50% occupancy. Had more extensive data been available, it might have been advantageous to include further positions at low occupancy. It is possible to select a reasonable route for the bridge through these disordered atoms (with
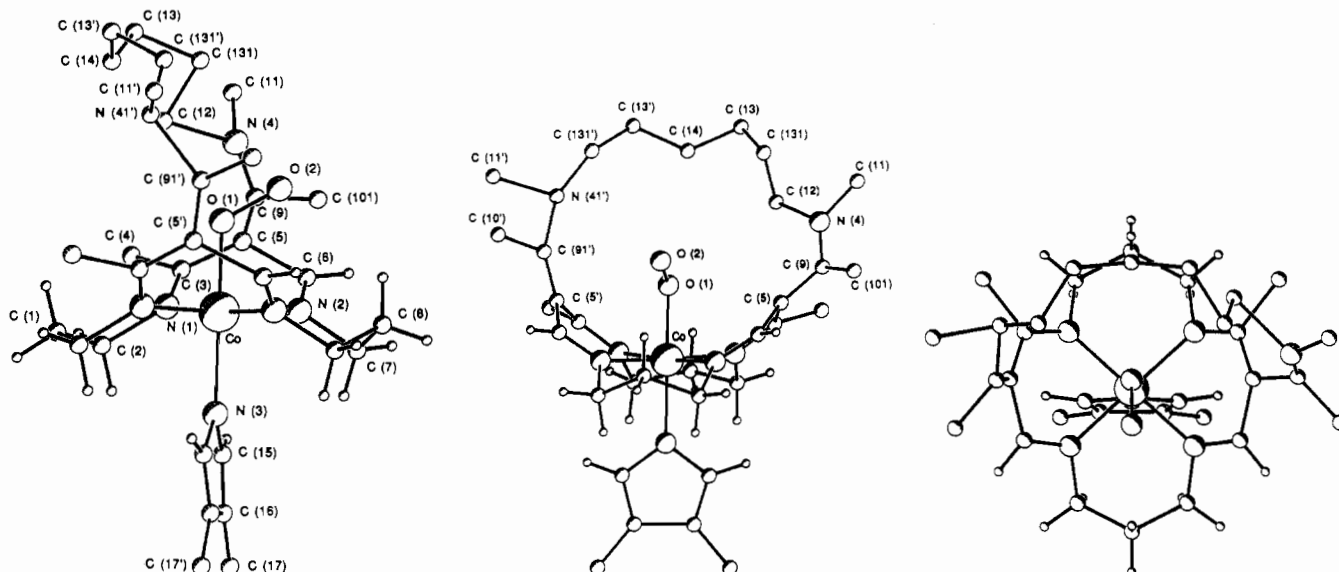
**Figure 3.** Structure of [Co(MeMeC6[16]cyclidene)(MeIm)(O₂)]²⁺: (a, left) side view showing the rising superstructure and bent Co–O–O unit; (b, center) front view looking into cavity; (c, right) view from above cavity.
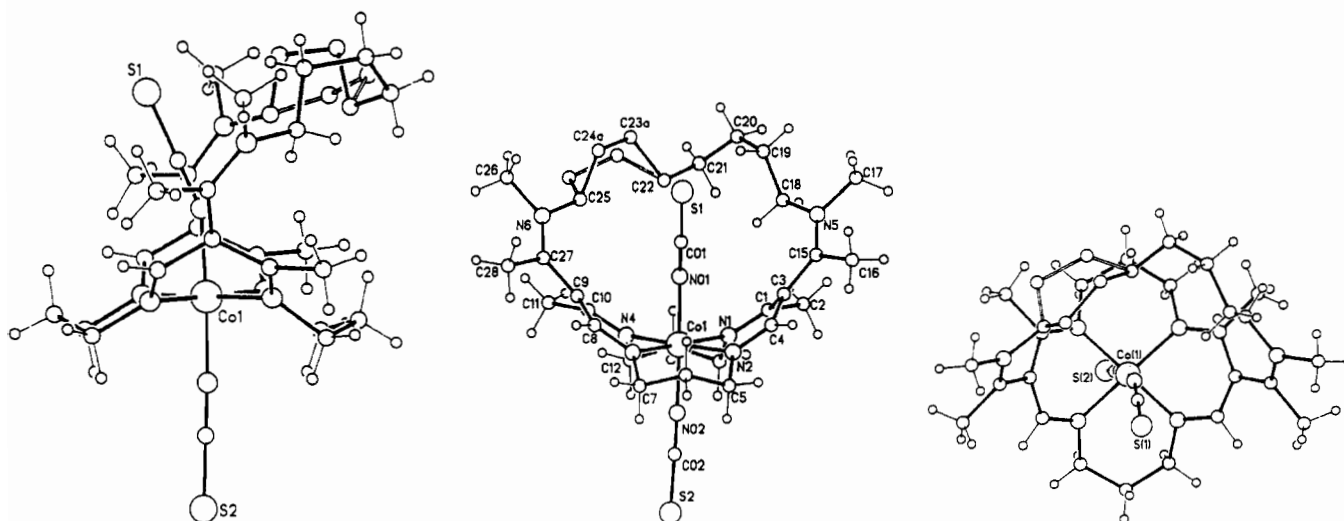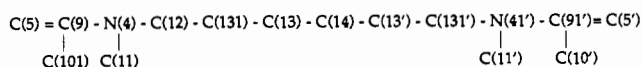


**Figure 4.** Structure of [Co(MeMeC8[16]cyclidene)(NCS)₂]⁺: (a, left) side view showing the open superstructure and bent Co–N–C–S unit; (b, center) front view looking into cavity; (c, right) view from above cavity.

primed atoms related to unprimed ones by the mirror plane):

C(5) = C(9) - N(4) - C(12) - C(131) - C(13) - C(14) - C(13') - C(131') - N(41') - C(91')= C(5')
     |         |                                                                   |          |
   C(101)   C(11)                                                               C(11')    C(10')

This chain is used in the figures, to give a clear impression of the bridge arrangement. However, as well as the alternative conformation with this chain in its reversed (mirror-related) form, other chain arrangements certainly contribute to the structure as observed.

In view of the space group ambiguity, the possibility of the crystals being noncentrosymmetric was carefully examined by attempted refinement in space group $Pn2_1a$, without significant improvement. The observed pattern of high thermal parameters is in fact more consistent with disorder than with pseudosymmetry. The atoms on the mirror plane, including those of the O₂ ligand, show no anomalies; while the fluorine atoms of the PF₆⁻ group have fairly high thermal motion, their $U$ values are typical of those found in the many complexes of this type which have been studied. These values give no indication that the PF₆⁻ group represents the superposition of two inequivalent images. Final refinement was on $F$ by cascaded least-squares methods, for 139 parameters. The largest peak on a final difference Fourier synthesis was of height 0.8 e Å⁻³, in the vicinity of the disordered bridge. A weighting scheme of the form $w = 1/(\sigma^2(F) + gF^2)$ with $g = 0.012$ was used and shown to be satisfactory by a weight analysis. Maximum shift/error for final cycle = 0.4. Final $R = 0.126$ and $R_w = 0.138$, relatively high figures which can readily be understood in light of the weakly diffracting crystal and

the severe disorder. Computing was with SHELXTL on a Data General DG30; scattering factors in the analytical form and anomalous dispersion factors were from the *International Tables* (1974). The data collection parameters are summarized in Table 1. Final atomic coordinates appear in Table 2 and selected bond lengths and angles in Table 3.

**X-ray Data for [Co(MeMeC8)(SCN)₂]PF₆·H₂O.** The crystals examined were well-formed deep red blocks. Data were collected with a Nicolet P2₁ four-circle diffractometer in the $\omega$–$2\theta$ mode. Maximum $2\theta$ was 50° with scan range ±0.6° ($2\theta$) around the K$\alpha_1$–K$\alpha_2$ angles, and scan speed was 5–29° min⁻¹, depending on the intensity of a 2-s prescan; backgrounds were measured at each end of the scan for 0.25 of the scan time. $hkl$ ranges: 0/14; 0/15; −16/15. Three standard reflections were monitored every 200 reflections and showed no change during data collection. Unit cell dimensions and standard deviations were obtained by a least-squares fit to 15 reflections (18 < $2\theta$ < 20°). Reflections were processed using profile analysis to give 6761 unique reflections, of which 5011 were considered observed ($I/\sigma(I) \geq 2.0$). These were corrected for Lorentz, polarization, and absorption effects (by the Gaussian method); minimum and maximum transmission factors were 0.78 and 0.90. Crystal dimensions were 0.28 × 0.52 × 0.39 mm.

No systematic reflection conditions were observed, and the space group P1̄ was chosen and shown to be correct by successful refinement. The cobalt atom was located by the Patterson interpretation section of SHELXTL PLUS, and the light atoms were then found by successive Fourier syntheses. A peak of height 4 e Å⁻³ was interpreted as an adventitious water molecule. Two atoms in the polymethylene chain

**Table 4.** Atom Coordinates ($\times 10^4$) and Isotropic Thermal Parameters ($\text{Å}^2 \times 10^3$) for [Co(MeMeC8)(SCN)$_2$]PF$_6$·H$_2$O

| atom | x | y | z | $u^a$ |
|------|------|------|------|------|
| Co(1) | 283.7(6) | 1424.2(6) | 3042.1(5) | 31(1)* |
| P(1) | 3066.9(15) | 6716.6(15) | 331.2(14) | 59(1)* |
| F(1) | 2801(5) | 6519(5) | 1317(3) | 108(3)* |
| F(2) | 3324(4) | 6815(6) | −706(4) | 120(3)* |
| F(3a) | 4281(6) | 6437(12) | 599(7) | 148(7)* |
| F(4a) | 3463(11) | 8026(6) | 1137(8) | 179(6)* |
| F(5a) | 1899(7) | 7146(10) | 128(6) | 131(5)* |
| F(6a) | 2541(10) | 5433(5) | −362(5) | 137(5)* |
| F(3b) | 4200(19) | 7539(25) | 793(19) | 57(8) |
| F(4b) | 2684(31) | 7868(23) | 597(27) | 72(10) |
| F(5b) | 1822(21) | 6138(35) | −222(25) | 82(11) |
| F(6b) | 3660(30) | 5631(24) | 108(27) | 75(10) |
| S(1) | 3006(2) | 4738(2) | 4403(2) | 85(1)* |
| S(2) | −3192(2) | −1072(2) | 1705(2) | 103(1)* |
| N(01) | 1649(3) | 2543(4) | 3562(3) | 36(2)* |
| N(02) | −1110(4) | 376(4) | 2522(3) | 47(2)* |
| C(01) | 2191(5) | 3457(5) | 3915(4) | 42(2)* |
| C(02) | −1977(5) | −217(5) | 2187(4) | 48(2)* |
| O(001) | 1485(9) | 6048(9) | 2948(8) | 180(4) |
| N(1) | 905(3) | 540(4) | 3862(3) | 35(2)* |
| N(2) | −275(4) | 2331(4) | 4261(3) | 39(2)* |
| N(3) | −318(4) | 2313(4) | 2262(3) | 41(2)* |
| N(4) | 879(4) | 515(4) | 1823(3) | 37(2)* |
| N(5) | 3219(5) | 2924(5) | 6600(4) | 63(2)* |
| N(6) | 3064(4) | 2882(4) | 1136(4) | 51(2)* |
| C(1) | 1407(4) | 1021(5) | 4834(4) | 34(2)* |
| C(2) | 1889(5) | 290(5) | 5405(4) | 45(2)* |
| C(3) | 1347(4) | 2228(5) | 5469(4) | 38(2)* |
| C(4) | 335(5) | 2666(5) | 5190(4) | 42(2)* |
| C(5) | −1369(5) | 2777(6) | 4152(5) | 57(3)* |
| C(6) | −1393(6) | 3493(6) | 3488(5) | 59(3)* |
| C(7) | −1403(5) | 2766(6) | 2376(5) | 57(3)* |
| C(8) | 263(5) | 2622(5) | 1670(4) | 41(2)* |
| C(9) | 1229(4) | 2156(5) | 1348(4) | 38(2)* |
| C(10) | 1337(4) | 971(5) | 1257(4) | 36(2)* |
| C(11) | 1827(6) | 231(5) | 357(4) | 50(2)* |
| C(12) | 739(5) | −767(5) | 1526(4) | 47(2)* |
| C(13) | 1292(6) | −1110(5) | 2379(4) | 51(2)* |
| C(14) | 738(5) | −750(4) | 3310(4) | 43(2)* |
| C(15) | 2116(6) | 2947(5) | 6422(4) | 50(2)* |
| C(16) | 1650(8) | 3773(8) | 7290(5) | 93(4)* |
| C(17) | 3941(8) | 3591(9) | 7653(6) | 100(4)* |
| C(18) | 3860(7) | 2275(9) | 5828(6) | 100(5)* |
| C(19) | 4896(8) | 2861(11) | 5741(10) | 133(7)* |
| C(20) | 5616(9) | 2012(12) | 5099(12) | 154(10)* |
| C(21) | 5244(16) | 1137(15) | 4076(12) | 202(7) |
| C(22) | 4628(15) | 1512(15) | 3396(13) | 179(6) |
| C(23a) | 5415(15) | 2338(18) | 3044(15) | 78(5) |
| C(24a) | 4754(16) | 3031(16) | 2499(14) | 85(6) |
| C(23b) | 5263(22) | 1519(27) | 2536(23) | 143(9) |
| C(24b) | 4544(13) | 1763(13) | 1557(12) | 78(5) |
| C(25) | 3709(6) | 2424(9) | 1836(7) | 88(5)* |
| C(26) | 3783(7) | 3557(8) | 730(6) | 77(4)* |
| C(27) | 1952(5) | 2841(5) | 988(4) | 46(2)* |
| C(28) | 1434(6) | 3550(7) | 418(6) | 68(3)* |

$^a$ Asterisks indicate equivalent isotropic $U$ defined as one-third of the trace of the orthogonalized $\mathbf{U}_{ij}$ tensor.

**Table 5.** Selected Bond Lengths (Å) and Angles (deg) for [Co(MeMeC8)(SCN)$_2$]PF$_6$·H$_2$O

| | | | |
|------|------|------|------|
| Co(1)–N(O1) | 1.907(4) | Co(1)–N(O2) | 1.890(5) |
| Co(1)–N(1) | 1.972(5) | Co(1)–N(2) | 1.938(4) |
| Co(1)–N(3) | 1.928(6) | Co(1)–N(4) | 1.964(4) |
| S(1)–C(O1) | 1.634(6) | S(2)–C(O2) | 1.614(6) |
| N(O1)–C(O1) | 1.145(7) | N(O2)–C(O2) | 1.143(7) |
| N(1)–C(1) | 1.294(6) | N(1)–C(14) | 1.475(6) |
| N(2)–C(4) | 1.292(7) | N(2)–C(5) | 1.474(8) |
| N(3)–C(7) | 1.469(8) | N(3)–C(8) | 1.313(8) |
| N(4)–C(10) | 1.302(8) | N(4)–C(12) | 1.470(7) |
| N(5)–C(15) | 1.313(9) | N(5)–C(17) | 1.485(8) |
| N(5)–C(18) | 1.470(10) | N(6)–C(25) | 1.462(12) |
| N(6)–C(26) | 1.477(12) | N(6)–C(27) | 1.312(8) |
| C(1)–C(2) | 1.510(9) | C(1)–C(3) | 1.445(7) |
| C(3)–C(4) | 1.427(8) | C(3)–C(15) | 1.427(7) |
| C(5)–C(6) | 1.511(12) | C(6)–C(7) | 1.495(9) |
| C(8)–C(9) | 1.407(8) | C(9)–C(10) | 1.443(8) |
| C(9)–C(27) | 1.443(9) | C(10)–C(11) | 1.510(8) |
| C(12)–C(13) | 1.498(9) | C(13)–C(14) | 1.511(9) |

| | | | |
|------|------|------|------|
| N(O1)–Co(1)–N(O2) | 177.1(2) | N(O1)–Co(1)–N(1) | 91.2(2) |
| N(O2)–Co(1)–N(1) | 91.3(2) | N(O1)–Co(1)–N(2) | 88.8(2) |
| N(O2)–Co(1)–N(2) | 89.9(2) | N(1)–Co(1)–N(2) | 85.8(2) |
| N(O1)–Co(1)–N(3) | 88.2(2) | N(O2)–Co(1)–N(3) | 89.3(2) |
| N(1)–Co(1)–N(3) | 179.0(2) | N(2)–Co(1)–N(3) | 93.4(2) |
| N(O1)–Co(1)–N(4) | 90.2(2) | N(O2)–Co(1)–N(4) | 91.1(2) |
| N(1)–Co(1)–N(4) | 93.7(2) | N(2)–Co(1)–N(4) | 178.9(2) |
| N(3)–Co(1)–N(4) | 87.1(2) | C(10)–N(4)–C(12) | 119.5(4) |
| Co(1)–N(O1)–C(O1) | 156.7(5) | Co(1)–N(O2)–C(O2) | 176.4(6) |
| S(1)–C(O1)–N(O1) | 177.8(5) | S(2)–C(O2)–N(O2) | 179.1(5) |
| C(7)–N(3)–C(8) | 116.8(6) | C(15)–N(5)–C(18) | 125.7(5) |
| Co(1)–N(4)–C(12) | 116.3(4) | C(25)–N(6)–C(26) | 114.1(6) |
| C(15)–N(5)–C(17) | 120.7(6) | C(26)–N(6)–C(27) | 122.0(6) |
| C(17)–N(5)–C(18) | 113.6(6) | N(1)–C(1)–C(3) | 121.7(5) |
| C(25)–N(6)–C(27) | 123.3(6) | C(1)–C(3)–C(4) | 116.0(4) |
| N(1)–C(1)–C(2) | 121.2(5) | C(4)–C(3)–C(15) | 117.4(5) |
| C(2)–C(1)–C(3) | 116.2(4) | N(2)–C(5)–C(6) | 111.2(6) |
| C(1)–C(3)–C(15) | 125.9(5) | N(3)–C(7)–C(6) | 111.2(5) |
| N(2)–C(4)–C(3) | 125.4(5) | C(8)–C(9)–C(10) | 118.1(5) |
| C(5)–C(6)–C(7) | 112.8(6) | C(10)–C(9)–C(27) | 124.5(5) |
| N(3)–C(8)–C(9) | 125.4(6) | N(4)–C(10)–C(11) | 121.6(5) |
| C(8)–C(9)–C(27) | 116.7(5) | N(4)–C(12)–C(13) | 112.9(4) |
| N(4)–C(10)–C(9) | 121.3(5) | N(1)–C(14)–C(13) | 111.6(5) |
| C(9)–C(10)–C(11) | 116.3(5) | N(5)–C(15)–C(16) | 117.1(5) |
| C(12)–C(13)–C(14) | 113.7(5) | N(5)–C(15)–C(3) | 123.9(5) |
| C(3)–C(15)–C(16) | 119.0(6) | | |

+0.9 and −0.6 e $\text{Å}^{-3}$, the largest peaks were near the polymethylene chain, and the high thermal parameters of some of these atoms indicate the likelihood of some additional disorder.

A weighting scheme of the form $w = I/(\sigma^2(F) + gF^2)$ with $g = 0.0015$ was used and shown to be satisfactory by a weight analysis. Maximum shift/error in final cycle = 0.5. Computing was performed with SHELXTL PLUS (Sheldrick, 1986) on a DEC Microvax-11.12; scattering factors in the analytical form and anomalous-dispersion factors were taken from the *International Tables* (1974).[13] The data collection parameters are summarized in Table 1. Final atomic coordinates are given in Table 4 and selected bond lengths and angles in Table 5.

## Results and Discussion

The central theme of this paper is how variations in ligand structure affect the dioxygen-binding properties of cobalt(II) [16]-cyclidene complexes. In the first section to follow, the results of X-ray crystal structure determinations are presented for two cobalt [16]cyclidene complexes that are especially important to this subject. These structures are used to complete the structural fabric of cyclidene dioxygen carrier chemistry. Thereafter, attention is given to the effect of the bridging group, R$^1$, in determining the dioxygen affinities, a subject that has been partially examined in earlier publications.[2b,5a,6b,c] In the next section, the effects of changes in R$^2$ and R$^3$ and influence of solvent and axial ligand are examined. Finally, a detailed analysis is presented for the ESR spectra of the cobalt cyclidene dioxygen adducts.

Some 20 different cobalt(II) cyclidenes were prepared, characterized, and studied in this work. The syntheses followed the

(C(23) and C(24)) appeared with alternate positions, which were given coupled occupational parameters (refined values: 0.47(2), positions (a); 0.53, positions (b)); at a late stage in refinement, four of the largest residual peaks were observed to lie in the equatorial plane around the F(1)–P–F(2) axis, between the four fluorine atoms with highest thermal parameters. These were included as additional part-occupancy atoms, with coupled parameters (refined to 0.84(1) for the principal positions and 0.16 for the minor ones); a soft constraint was applied to the equatorial P–F distances (1.53(3) Å). Anisotropic thermal parameters were used for all non-H atoms, apart from the solvent water, the disordered chain atoms, and the minor fluorine atoms. Hydrogen atoms were given fixed isotropic thermal parameters, $U = 0.08$ Å$^2$. Those defined by the molecular geometry were inserted at calculated positions and not refined (excluding those on the disordered chain atoms and the adjacent atoms); methyl groups were refined as rigid Me units. Final refinement was on $F$ by least-squares methods refining 461 parameters. Largest positive and negative peaks on a final difference Fourier synthesis were of heights

**Table 6.** Elemental Analysis Data for Cobalt(II) [16]Cyclidene Complexes

| $R^3$ | $R^2$ | $R^1$ | formula | % calcd | | | | % found | | | |
|---|---|---|---|---|---|---|---|---|---|---|---|
| | | | | C | H | N | Co | C | H | N | Co |
| Ph | H | C4 | $C_{36}H_{49}N_7OP_2F_{12}Co$ | 45.77 | 5.23 | 10.38 | 6.24 | 45.63 | 5.37 | 10.28 | 6.09 |
| Me | Me | C4 | $C_{24}H_{40}N_6P_2F_{12}Co$ | 37.86 | 5.30 | 11.04 | | 38.16 | 5.47 | 11.17 | |
| Ph | Me | C4 | $C_{34}H_{44}N_6P_2F_{12}Co$ | 46.11 | 5.01 | 9.50 | 6.68 | 46.11 | 5.19 | 9.63 | 6.45 |
| Me | H | C5 | $C_{23}H_{38}N_6P_2F_{12}Co$ | 36.96 | 5.12 | 11.24 | 7.88 | 36.79 | 5.13 | 11.21 | 7.62 |
| Ph | H | C5 | $C_{33}H_{42}N_6P_2F_{12}Co$ | 45.48 | 4.86 | 9.64 | 6.76 | 45.20 | 5.06 | 9.87 | 6.58 |
| Me | Me | C5 | $C_{25}H_{42}N_6P_2F_{12}Co$ | 38.72 | 5.46 | 10.84 | 7.60 | 38.67 | 5.66 | 10.64 | 7.49 |
| Ph | Me | C5 | $C_{35}H_{46}N_6P_2F_{12}Co$ | 44.77 | 5.00 | 9.29 | 6.27 | 44.78 | 5.56 | 8.92 | 6.04 |
| Me | $PhCH_2$ | C6 | $C_{38}H_{52}N_6P_2F_{12}Co$ | 48.40 | 5.53 | 8.93 | 6.27 | 48.50 | 5.69 | 9.44 | 6.27 |
| Me | H | C6 | $C_{24}H_{40}N_6P_2F_{12}Co$ | 37.86 | 5.30 | 11.04 | | 37.77 | 5.32 | 11.48 | |
| Ph | H | C6 | $C_{34}H_{44}N_6P_2F_{12}Co$ | 46.11 | 5.01 | 9.49 | 6.65 | 45.83 | 5.20 | 9.26 | 6.52 |
| t-Bu | H | C6 | $C_{30}H_{52}N_6P_2F_{12}Co$ | 42.61 | 6.20 | 9.94 | 6.97 | 42.67 | 6.34 | 9.98 | 6.84 |
| H | Me | C6 | $C_{26}H_{43}N_7P_2F_{12}Co$ | 38.91 | 5.40 | 12.22 | 7.34 | 39.00 | 5.72 | 11.94 | 7.40 |
| Me | Me | C6 | $C_{26}H_{44}N_6P_2F_{12}Co$ | 39.55 | 5.62 | 10.64 | 7.46 | 39.53 | 5.70 | 10.76 | 7.43 |
| n-Bu | Me | C6 | $C_{34}H_{59}N_7P_2F_{12}Co$ | 44.64 | 6.46 | 10.72 | 6.53 | 44.92 | 6.51 | 11.04 | 6.80 |
| n-Pr | Me | C6 | $C_{30}H_{52}N_6P_2F_{12}Co$ | 42.61 | 6.20 | 9.94 | 6.97 | 43.88 | 6.31 | 9.81 | 7.62 |
| Ph | Me | C6 | $C_{36}H_{48}N_6P_2F_{12}Co$ | 47.33 | 5.30 | 9.20 | 6.45 | 47.29 | 5.40 | 9.01 | 6.28 |
| Me | H | C7 | $C_{29}H_{48}N_8P_2F_{12}Co$ | 40.62 | 5.64 | 13.07 | 6.87 | 40.61 | 5.79 | 13.01 | 7.25 |
| Me | Me | C7 | $C_{27}H_{46}N_6P_2F_{12}Co$ | 40.36 | 5.77 | 10.46 | 7.33 | 40.53 | 5.96 | 10.60 | 7.11 |
| Ph | Me | C7 | $C_{37}H_{50}N_6P_2F_{12}Co$ | 47.90 | 5.43 | 9.06 | 6.35 | 47.51 | 5.53 | 9.23 | 6.04 |
| Me | H | C8 | $C_{26}H_{44}N_6P_2F_{12}Co$ | 39.55 | 5.62 | 10.64 | 7.46 | 39.81 | 5.69 | 10.59 | 7.56 |
| Me | Me | C8 | $C_{29}H_{52}N_6P_2F_{12}Co$ | 41.00 | 6.17 | 9.89 | 6.94 | 40.69 | 6.11 | 9.87 | 6.94 |

**Table 7.** O–O Bond Distances and Values for the Co–O–O Angle[a]

| Compound | O–O Å | Co–O–O, deg |
|---|---|---|
| $Co(bzacen)pyO_2$ | 1.26(8) | 126(4) |
| $Co(salen)(C_2H_4py)O_2$ | 1.1(1) | 136 |
| $[Co(CN)_5O_2]^{3-}$ | 1.24(2) | 153(2) |
| $Co(t\text{-}Bu\text{-}salten)(bzIm)O_2$ | 1.27(1) | 117.5(6) |
| $Co(3\text{-}F\text{-}saltmen)(N\text{-}Mim)O_2$ | 1.320(3) | 117.4(2) |
| $Co(saltmen)(N\text{-}bzylIm)O_2$ | 1.277(3) | 120.0(2) |
| $Co(3\text{-}MeO\text{-}saltmen)(aqua)O_2$ | 1.25(2) | 117(1) |
| $Co(3\text{-}t\text{-}Bu\text{-}salen)pyO_2$ | 1.350(11) | 116.4(5) |
| this work | 1.32(2) | 121(1) |
| $\alpha\text{-}KO_2$ | 1.28 | |
| $\beta\text{-}NaO_2$ | 1.31 | |
| $BaO_2$ | 1.48 | |

[a] Schaefer, W. P.; Huie, B. T.; Kurilla, M. G.; Ealick, S. E. *Inorg. Chem.* **1980**, *19*, 340 and references therein.

general preparative schemes described previously.[10] In each case, the ligand was fashioned in a template reaction about a nickel-(II) center. After demetalation with HCl or HBr gas and isolation of the ligand salt, the cobalt(II) complex was prepared by mixing the ligand salt with methanolic cobalt(II) acetate under mildly basic conditions, in an inert-atmosphere enclosure. Analytical data for the nickel(II) complexes have been published,[16] and those for the cobalt(II) complexes are summarized in Table 6. The complexes reported here are the most typical and best behaved of the cyclidene family, and the structural relationships are most straightforward. The bridging group $(CH_2)_n$, where $n = 4$–8, defines the subfamily of cyclidene complexes that dominate the discussion that follows.

**Crystal Structures of $[Co(MeMeC6)(1\text{-}MeIm)(O_2)](PF_6)_2$ and $[Co(MeMeC8)(NCS)_2]PF_6$.** The X-ray crystal structure of $[Co(MeMeC6)(1\text{-}MeIm)(O_2)](PF_6)_2$ has been successfully solved despite disorder in the C6 bridge as described in the Experimental Section. The structure has been clearly defined; in particular, the crucial parameters of the bound dioxygen are well-determined, as may be seen in the diagrams shown in Figure 3. Some of the features of this structure have been discussed previously.[9c] The structure of the ligand is typical for a six-coordinate [16]cyclidene complex, with the saturated rings in the boat form. The $R^1$ bridge

in the five-coordinate cyclidene resides over the cavity whereas, in complexes with a six-coordinate cobalt, the bridging group is pushed back away from the cavity. A similar conformational change was observed previously for the X-ray structure of the analogous $[Co(MeMeC6)(SCN)_2]PF_6$ complex.[17] The position of the C6 bridge is clear, despite its disorder. It is bent well back from the Co–O axis, with a "lid-off" configuration at the bridgehead nitrogen N(4).[18] The bridge therefore blocks the rear of the complex, leaving the coordinated dioxygen projecting to the front. Extreme disorder is characteristic of C6-bridged cyclidenes and is found, for example, in the analogous cobalt(III) bis(thiocyanato) cyclidene complex.[17] The factors controlling the conformations of the polymethylene bridge in five-coordinate and six-coordinate cyclidene complexes were discussed in more detail previously.[9] The C6 chain is shown in a unique orientation (see text), but both positions for the disordered methyl group of the bound N-methylimidazole are included. The O–O distance of 1.32(2) Å and Co–O–O angle of 121(1)° are typical for 1:1 cobalt–dioxygen adducts, as may be seen by comparison with data for other dioxygen adducts, listed in Table 7.

From the crystal structure it is apparent that the dioxygen is coordinated end-on to the cobalt(II), as first suggested for hemoglobin by Pauling.[19] The coordinated dioxygen O–O bond length is longer than that of free dioxygen (1.208 Å)[20] and close to that of free gaseous superoxide (1.34 Å).[21] This conclusion supports the conventional view, based on infrared and UV–visible studies, that the coordinated dioxygen in the cobalt cyclidene complexes is best described as a coordinated superoxide.[22]

Four crystal structures have been determined on C6-bridged [16]cyclidene complexes (including that described immediately above), two with the cavity occupied and two with the cavity vacant.[9a,c] These studies and molecular mechanics studies have revealed that the C6 bridge has two distinct dominant low-energy conformations. One conformation folds the central carbons of the polymethylene chain back into the region of the cavity, greatly diminishing the cavity volume, and is well suited to the vacant cavity. The second conformation folds the central carbons out
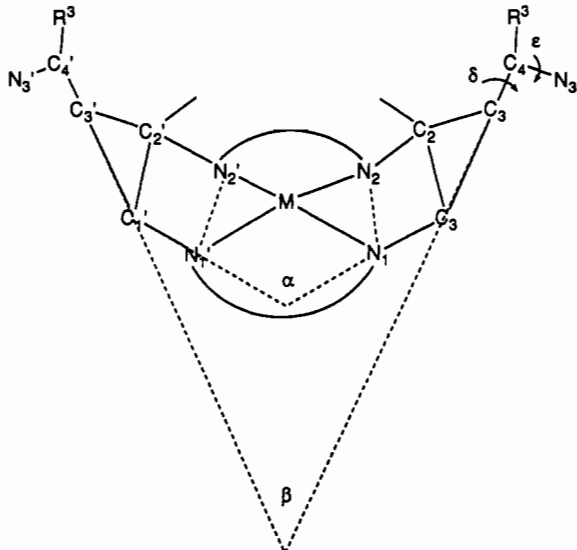
(16) (a) Korybut-Daszkiewicz, B.; Kojima, M.; Cameron, J. H.; Herron, H.; Chavan, M. Y.; Jircitano, A. J.; Coltrain, B. K.; Neer, G. L.; Alcock, N. W.; Busch, D. H. *Inorg. Chem.* **1984**, *23*, 903. (b) Busch, D. H.; Olszanski, D. J.; Stevens, J. C.; Schammel, W. P.; Kojima, M.; Herron, N.; Zimmer, L. L.; Holter, K. A.; Mocak, J. *J. Am. Chem. Soc.* **1981**, *103*, 1472. (c) Busch, D. H.; Jackels, S. C.; Callahan, R. C.; Grzybowski, J. J.; Zinner, M.; Olszanski, D. J.; Schammel, W. P.; Stevens, J. C.; Holter, K. A.; Mocak, J. *Inorg. Chem.* **1981**, *20*, 2834.

(17) Stevens, J. C.; Jackson, P. J.; Schammel, W. P.; Christoph, G. G.; Busch, D. H. *J. Am. Chem. Soc.* **1980**, *102*, 3283.

(18) Herron, N.; Nosco, D. L.; Busch, D. H. *Inorg. Chem.* **1983**, *22*, 2970.

(19) (a) Pauling, L. *Standford Med. Bull.* **1948**, *6*, 215. (b) Pauling, L. *Nature (London)* **1964**, *203*, 182.

(20) *CRC Handbook of Chemistry and Physics*, 61st ed.; Weast, R. C., Astle, M. J., Eds.; CRC Press Inc.: Boca Raton, FL, 1980.

(21) Celotta, R. L.; Bennett, R. A.; Hall, J. R.; Siegel, M. W.; Levine, J. *Phys. Rev. A* **1972**, *6*, 631.

(22) Masarwa, M.; Sauer-Masarwa, A.; Ye, N.; Busch, D. H. *J. Coord. Chem.* **1993**, *28*, 355.

**Table 8.** Selected Infrared Data for $[Co(MeMeR^1[16]cyclidene)(NCS)_2]PF_6$ Complexes

| $R^1$ | $\nu_{C\equiv N}$, cm$^{-1}$ | $\nu_{C=N}$, cm$^{-1}$ | condition | Co–N, Å | | Co–N–C, deg | |
|---|---|---|---|---|---|---|---|
| | | | | inside | outside | inside | outside |
| $(CH_2)_5{}^a$ | 2110, 2045 | 1620 | $CH_3CN$ | 1.940(4) | 1.900(4) | 140.8(4) | 156.6(5) |
| $(CH_2)_6{}^a$ | 2100, 2050 | 1620 | $CH_3CN$ | 1.94(1) | 1.88(1) | 148.5(1) | 172.3(11) |
| $(CH_2)_7{}^a$ | 2102, 2032 | 1620 | $CH_3CN$ | | | | |
| $(CH_2)_8$ | 2105 | 1620 | $CH_3CN$ | 1.907(4) | 1.890(5) | 156.7(5) | 176.4(6) |
| $(CH_2)_8$ | 2103 | 1617 | KBr | | | | |
| $(CH_2)_{11}{}^b$ | 2101 | 1617 | KBr | 1.891(3) | 1.881(8) | 156.4(7) | 166.0(8) |

$^a$ Jackson, P. J.; Cairns, C.; Lin, W. K.; Alcock, N. W.; Busch, D. H. *Inorg. Chem.* **1986**, *25*, 4015. $^b$ Chia, P. S.; Masarwa, M.; Warburton, P. R.; Wu, W.; Kojima, M.; Nosco, D.; Alcock, N. W.; Busch, D. H. *Inorg. Chem.* **1993**, *32*, 2736.

**Table 9.** Cavity Widths for the Complexes $[Co(MeMeCn[16]cyclidene(NCS)_2]^+$



| complex | $\alpha$, deg | $\beta$, deg | $C_4$–$C_4'$, Å | $N_3$–$N_3'$, Å | Co–N–C, deg |
|---|---|---|---|---|---|
| $-(CH_2)_5-{}^a$ | 105.6 | 49.3 | 6.76 | 6.46 | 140.8 |
| $-(CH_2)_6-{}^b$ | 108.8 | 51.4 | 7.09 | 6.92 | 148.5 |
| $-(CH_2)_8-$ | 112.0 | 64.1 | 7.62 | 7.69 | 156.7 |
| $-(CH_2)_{11}-{}^c$ | 110.9 | 61.9 | 7.51 | 7.56 | 157.0 |

$^a$ Stevens, J. C.; Jackson, P. J.; Cairns, C.; Lin, W.-K.; Alcock, N. W.; Busch, D. H. *Inorg. Chem.* **1986**, *25*, 4015. $^b$ Jackson, P. J.; Schammel, W. P.; Christoph, G. C.; Busch, D. H. *J. Am. Chem. Soc.* **1980**, *102*, 3283. $^c$ Chia, P. S.; Masarwa, M.; Warburton, P. R.; Wu, W.; Kojima, M.; Nosco, D.; Alcock, N. W.; Busch, D. H. *Inorg. Chem.* **1993**, *32*, 2736.

away from the cavity, maximizing cavity volume and optimizing it for occupancy. Our molecular mechanics studies led us to predict the same *dual-conformation* behavior for the heptamethylene and octamethylene structures.[9a] The crystal structure of the C8-bridged cobalt [16]cyclidene complex $[Co(MeMeC8)-(SCN)_2]PF_6$ allows us to test this hypothesis. Prior to this work, crystal structures of the bis(thiocyanato)cobalt(III) cyclidenes with polymethylene bridges containing 5, 6, and 11 methylene units were published.[10b,17,23] As mentioned above, the bridge length C*n* of the cobalt(II) cyclidenes with $R^2 = R^3 = Me$ determines the width of the ligand cavity, which in turn regulates the dioxygen affinity. The dioxygen affinity and cavity width increase with bridge length up to $n = 8$ and decrease thereafter.

The mass spectrum (FAB/NBA) of the bis(thiocyanato) complex exhibited three major peaks at $m/z$ 643 $(CoL(SCN)_2)^+$, 585 $(CoL(SCN))^+$, and 526 $(CoL + H)^+$. The $^{13}C$ NMR spectrum of $[Co^{III}(MeMeC8)(NCS)_2]PF_6$ with two resonances at 140.1 and 142.0 ppm is consistent with two different NCS carbons. The infrared spectrum of $[Co^{III}(MeMeC8)(NCS)_2]-PF_6$ has a band corresponding to the $(SCN^-)$ $N\equiv C$ stretching

vibration (ca. 2100 cm$^{-1}$). A comparison of this infrared spectrum with those of the analogous cyclidene complexes with $R^1$ of different lengths is presented in Table 8. The solution infrared spectra of similar complexes with shorter bridges ($R^1$ from $n = 5$ to 7) were found to show two $C\equiv N$ stretches at ca. 2105 and 2045 cm$^{-1}$, believed to belong to the two types of bound thiocyanates; one is more nearly linear and is bound outside the cavity, while the NCS$^-$ within the cavity has its cobalt–nitrogen bond axis more sharply bent, because of steric interactions with the bridge. In contrast, the infrared spectrum for the complex with $R^1 = C8$ shows only one band in the triple-bond region under both solid and solution conditions. For the previously reported complex having the long C11 bridge, the cavity is much higher; again, only a single CN triple-bond stretch is observed.[10b,17,23] In general, therefore, for long bridges, $R^1 = C8$–C12, the degree of bending of the Co–N–C bond is insufficient to differentiate between the internal and external NCS$^-$ ligands at modest infrared spectral resolutions.[23] Comparison of X-ray crystallographic data with infrared stretching frequencies (Table 8) shows that Co$^{III}$–N–C bond angles must be bent below about 156° in order to lower the CN stretching frequency appreciably. Remarkably, three compounds, two with the NCS in the cavity and one with it outside, have Co–N–C bond angles of 156.4–156.7° and all show stretching frequencies within a few wavenumbers of 2100 cm$^{-1}$. Conversely, the two cases in which the angles are below 150° display decreases in frequency of 50 and 55 cm$^{-1}$. Similarly, distortion of the Co–N–C bond angle by steric interaction with the cavity does not measurably affect the Co–N bond distance until the distortion reduces the bond angle below 150°. Thus, the splitting of the CN stretching frequency correlates with the elongation of the Co–N bond; i.e., both structures in which the stretching frequency is reduced have bond distances elongated by some 0.04 Å (Table 8).

The results of the crystal structure determination for $[Co^{III}-(MeMeC8)(NCS)_2]PF_6$ are shown in Figure 4. The coordination geometry about the cobalt is pseudooctahedral, with the saturated chelate rings of the $N_4$ macrocycle in a chair conformation. The unsaturated rings rise above the $N_4$ plane and provide the walls for the saddle-shaped cavity. The bridgehead nitrogens are in the lid-off configuration.[18] Table 9 compares the structural parameters pertinent to the cavity sizes of the known bis(thiocyanato) cyclidene adducts. The cavity width measured between the bridgehead nitrogens of the six-coordinate complex (N–N′ distance = 7.69 Å) is similar to that of the analogous four-coordinate complex with $n = 8$ (N–N′ distance = 7.82 Å)[9c] and also close to that of the six-coordinate complex with $n = 11$ (N–N′ = 7.56 Å).[10b] These results indicate that the 16-membered cyclidene complexes have a maximum cavity width of nearly 8 Å, which can be approached either by binding a small ligand inside the cavity or by an octamethylene bridge. The latter is worth noting because it suggests that the wide cavity of the octamethylene complex is *preorganized* for small ligand binding inside the cavity, and indeed, it has the highest dioxygen affinity in the series. Equally significant, the conformation of the bridging octamethylene group in the bis(thiocyanato) complex contrasts strongly with that of C8 complexes having vacant cavities. Whereas the latter have their central methylene groups folded

(23) Jackson, P. J.; Cairns, C.; Lin, W.-K.; Alcock, N. W.; Busch, D. H. *Inorg. Chem.* **1986**, *25*, 4015.

**Table 10.** Dioxygen Affinities for Lacunar $[Co(R^2R^3Cn[16]cyclidene)(MeIm)]^{2+}$ Complexes in Acetonitrile Containing 1.5 M 1-Methylimidazole

| $R^3$ | $R^2$ | $R^1$ | $T$, °C | $K_{O_2}$ | ref | $R^3$ | $R^2$ | $R^1$ | $T$, °C | $K_{O_2}$ | ref |
|---|---|---|---|---|---|---|---|---|---|---|---|
| Ph | H | C4 | −19.3 | 0.0018 | | n-Bu | Me | C6 | 20.0 | 0.23 | |
| Ph | H | C4 | −10.2 | 0.0011 | | n-Pr | Me | C6 | 20.0 | 0.24 | |
| Me | Me | C4 | −40 | 0.0020 | a | Ph | Me | C6 | 0 | 0.85 | c e |
| Ph | Me | C4 | −40 | 0.005 | | Ph | Me | C6 | 5.0 | 0.51 | |
| Me | H | C5 | −30 | 0.210 | | Ph | Me | C6 | 10.0 | 0.31 | |
| Me | H | C5 | −19.3 | 0.050 | | Ph | Me | C6 | 15.0 | 0.170 | |
| Me | H | C5 | −12.8 | 0.025 | | Ph | Me | C6 | 20.0 | 0.101 | |
| Me | H | C5 | −10.1 | 0.019 | a | Ph | Me | C6 | 25.0 | 0.065 | |
| Me | H | C5 | −0.6 | 0.0066 | | Ph | Me | C6 | 30.0 | 0.032 | |
| Ph | H | C5 | −10.2 | 0.017 | | Me | Me | C6[DM16]d | −2.4 | 1.0 | |
| Ph | H | C5 | −1.5 | 0.0079 | | Me | Me | C6[DM16]d | 0.0 | 0.86 | |
| Ph | H | C5 | 8.6 | 0.0026 | | Me | Me | C6[DM16]d | 9.2 | 0.27 | |
| Ph | H | C5 | 18.6 | 0.0012 | | Me | Me | C6[CM16]d | 17.6 | 0.16 | |
| Me | Me | C5 | −20 | 0.66 | | Me | Me | C6[DM16]d | 25.0 | 0.090 | |
| Me | Me | C5 | −10.1 | 0.215 | a b | Me | Me | C6[DM16DM]f | 20.0 | 0.170 | |
| Me | Me | C5 | 1.0 | 0.058 | | Me | H | C7 | −10.0 | 2.46 | |
| Me | Me | C5 | 10 | 0.019 | | Me | H | C7 | 0.0 | 0.80 | |
| Me | Me | C5 | 20 | 0.0094 | c | Me | H | C7 | 5.0 | 0.41 | |
| Ph | Me | C5 | −10 | 0.09 | | Me | H | C7 | 10.0 | 0.23 | |
| Ph | Me | C5 | 0 | 0.025 | | Me | H | C7 | 15.0 | 0.15 | |
| Ph | Me | C5 | 10 | 0.0097 | | Me | Me | C7 | 0.0 | 4.5 | |
| Ph | Me | C5 | 20 | 0.0031 | | Me | Me | C7 | 10.0 | 1.4 | |
| Ph | Me | C5 | 30 | 0.0015 | | Me | Me | C7 | 14.9 | 0.93 | |
| Me | Me | C5[DM16]d | −10 | 0.046 | | Me | Me | C7 | 19.4 | 0.62 | c |
| Me | Me | C2CMe2C2 | −20.0 | 0.102 | | Me | Me | C7 | 25.0 | 0.26 | |
| Me | Me | C2CMe2C2 | 0.0 | 0.027 | | Me | Me | C7 | 30.0 | 0.160 | |
| Me | Me | C2OC2 | 5.0 | 0.092 | | Ph | Me | C7 | 5 | 2.3 | |
| Me | Me | C2OC2 | 20.0 | 0.027 | | Ph | Me | C7 | 10 | 0.94 | |
| Me | PhCH2 | C6 | 20.0 | 0.144 | | Ph | Me | C7 | 15 | 0.51 | |
| Ph | PhCH2 | C6 | 5.6 | 0.54 | | Ph | Me | C7 | 20 | 0.27 | |
| Ph | PhCH2 | C6 | 20.0 | 0.13 | | Ph | Me | C7 | 25 | 0.16 | |
| Ph | PhCH2CH2 | C6 | 5.0 | 0.28 | | Me | H | C3NMeC3 | −20 | 0.114 | |
| Ph | PhCH2CH2 | C6 | 20.0 | 0.13 | | Me | H | C3NMeC3 | −15 | 0.053 | |
| Me | H | C6 | −19.3 | 1.7 | | Me | H | C3NMeC3 | −10 | 0.027 | |
| Me | H | C6 | −15 | 0.97 | | Me | H | C3NMeC3 | −5.0 | 0.016 | |
| Me | H | C6 | −10.1 | 0.49 | a | Me | H | C3NMeC3 | 0.0 | 0.0099 | |
| Me | H | C6 | 0 | 0.14 | c | Me | H | C3NMeC3 | 10 | 0.0064 | |
| Me | H | C6 | 2.1 | 0.12 | a | Me | H | C8 | 0.0 | 1.7 | |
| Ph | H | C6 | −10.0 | 1.3 | | Me | Me | C8 | 0.0 | 5.92 | |
| Ph | H | C6 | −5.0 | 0.64 | | Me | Me | C8 | 4.9 | 3.34 | |
| Ph | H | C6 | 1.0 | 0.41 | c | Me | Me | C8 | 10.0 | 1.95 | |
| Ph | H | C6 | 5.0 | 0.24 | | Me | Me | C8 | 15.0 | 1.13 | |
| Ph | H | C6 | 10.0 | 0.12 | | Me | Me | C8 | 20 | 0.65 | c |
| Ph | H | C6 | 15.0 | 0.071 | | Me | Me | C8 | 25.0 | 0.45 | |
| Ph | H | C6 | 20.0 | 0.025 | | Me | Me | C8 | 29.8 | 0.25 | |
| t-Bu | H | C6 | −0.4 | ~200 | c | Me | Me | C8[16DM]g | 20.0 | 1.75 | |
| H | Me | C6 | −25.0 | 0.16 | | Me | Me | C8[DM16]d | 12.1 | 1.2 | |
| H | Me | C6 | −20.0 | 0.083 | | Me | Me | Cy | −10.0 | 0.025 | |
| H | Me | C6 | −15.4 | 0.042 | | Me | Me | m-Xyl | −39.0 | 0.0019 | |
| H | Me | C6 | −10.0 | 0.026 | | Me | H | m-Xyl | −40.0 | 0.0085 | |
| H | Me | C6 | 0 | 0.010 | c | Me | Me | t-Bu-m-Xyl h | −34.7 | 0.010 | |
| Me | Me | C6 | −10.1 | 4.6 | a | Me | Me | CPhCPhC i | −4.4 | 1.2 | |
| Me | Me | C6 | 1.0 | 1.3 | a | Me | Me | CPhCPhC i | 6.3 | 0.33 | |
| Me | Me | C6 | 2.1 | 0.98 | c | Me | Me | CPhCPhC i | 9.2 | 0.23 | |
| Me | Me | C6 | 15 | 0.25 | c | Me | Me | CPhCPhC i | 15.5 | 0.14 | |
| Me | Me | C6 | 20.0 | 0.155 | a | Me | Me | CPhCPhC i | 20.3 | 0.70 | |

a Stevens, J. C.; Busch, D. H. *J. Am. Chem. Soc.* **1980**, *102*, 3285. b Misquoted in reference. c Busch, D. H. In *Oxygen Complexes and Oxygen Activation by Transition Metals*; Martell, A. E., Sawyer, D. T., Eds.; Plenum Press: New York, 1988. d *gem*-Dimethyl groups on saturated chelate ring at open side of lacuna. e Error in reference. f Two pairs of *gem*-dimethyl groups on saturated chelate rings. g *gem*-Dimethyl groups on saturated chelate ring at less open side of lacuna. h Bridge is 5-*tert*-butyl-*m*-xylylene. i Bridge is $-CH_2-m-C_6H_4-CH_2-m-C_6H_4-CH_2-$.

back into the cavity, this complex has a conformation in which the bridge projects its central carbons out and away from the cavity, in agreement with prediction (Figure 4).[9a]

**Effect of Bridge Length on the Dioxygen Affinity of Cobalt(II) Cyclidene Complexes at Constant $R^2$ and $R^3$.** As indicated earlier, the shortest bridge (trimethylene) fails to give dioxygen complexes[6b,c] while bridges longer than octamethylene lead to more extreme structural changes, which have been reported elsewhere.[9b,10b] Dioxygen affinities ($K_{O_2}$) were determined from changes in UV–visible spectra on varying the partial pressure of dioxygen. $K_{O_2}$ data are summarized in Tables 10 and 11. A small part of these data have been summarized and discussed briefly in preliminary reports.[2b,5] From van't Hoff plots of the

natural logarithm of the dioxygen affinity versus the inverse of temperature, selected enthalpies and the entropies of dioxygen binding have been determined and are summarized in Table 12.[2b]

The great variation in $K_{O_2}$ with changes in bridge length has been summarized in preliminary publications,[2b,5] but the effect is also shown here for a number of related series of lacunar cyclidenes differing in substituents $R^2$ and $R^3$. Figure 5 dramatizes this unusual structural control of a functional molecular parameter, showing clearly how the equilibrium constant varies over approximately 5 orders of magnitude as the bridge length changes. This figure summarizes the data for the three series for which four or five different chain lengths are available while all other structural variables are maintained

**Table 11.** Dioxygen Affinities for Lacunar $[Co(R^2R^3Cn[16]cyclidene)B]^{2+}$ Complexes in Various Solvent Systems

| $R^3$ | $R^2$ | $R^1$ | solvent | base | [B], M | $T$, °C | $K_{O_2}$ |
|---|---|---|---|---|---|---|---|
| Me | Me | C6 | acetone | py | 1 | −20 | 0.68 |
| Me | Me | C6 | acetone | py | 1 | −10 | 0.19 |
| Me | Me | C6 | MeCN | | | −20 | 0.026 |
| Me | Me | C6 | MeCN | | | −10 | 0.006 |
| Me | Me | C6 | MeCN | py | 1.5 | 0.0 | 0.065 |
| Me | Me | C6 | MeCN | py | 1.5 | 5.0 | 0.034 |
| Me | Me | C6 | MeCN | py | 1.5 | 10.0 | 0.020 |
| Me | Me | C6 | MeCN | py | 1.5 | 15.0 | 0.012 |
| Me | Me | C6 | DMF | | | −22.5 | 0.012 |
| Me | Me | C6 | DMF | MeIm | 2.5 | 1.0 | 2.8 |
| Me | Me | C6 | DMF | MeIm | 2.5 | 10.0 | 0.11 |
| Me | Me | C5 | $H_2O$ | MeIm | 2.5 | 4.8 | 0.17 |
| Me | Me | C5 | $H_2O$ | MeIm | 2.5 | 10 | 0.11 |
| Me | Me | C5 | $H_2O$ | MeIm | 2.5 | 15.3 | 0.055 |
| Me | Me | C5 | $H_2O$ | MeIm | 2.5 | 25 | 0.027 |
| Me | Me | C5 | $H_2O$ | MeIm | 2.5 | 29.8 | 0.013 |
| Me | Me | C5 | $H_2O$ | MeIm | 2.5 | 37 | 0.009 |
| Me | H | C6 | $H_2O$ | MeIm | 2.5 | 1.6 | 0.97 |
| Me | Me | C6 | $H_2O$ | MeIm | 2.5 | 3.3 | 7.7 |
| Me | Me | C6 | $H_2O$ | MeIm | 2.5 | 6.3 | 5.3 |
| Me | Me | C6 | $H_2O$ | MeIm | 2.5 | 8.3 | 4.8 |
| Me | Me | C6 | $H_2O$ | MeIm | 2.5 | 10 | 4.5 |
| Me | Me | C6 | $H_2O$ | MeIm | 2.5 | 14.8 | 2.2 |
| Me | Me | C6 | $H_2O$ | MeIm | 2.5 | 19.7 | 1.6 |
| Ph | Me | C6 | $H_2O$ | MeIm | 2.5 | 6.0 | 2.4 |
| Ph | Me | C6 | $H_2O$ | MeIm | 2.5 | 6.6 | 2.3 |
| Ph | Me | C6 | $H_2O$ | MeIm | 2.5 | 14.0 | 0.74 |
| Me | Me | C7 | MeCN | MeIm | 0.15 | 2.3 | 1.7 |
| Me | Me | C7 | MeCN | MeIm | 0.15 | 5.0 | 1.4 |
| Me | Me | C7 | MeCN | MeIm | 0.15 | 8.4 | 1.0 |
| Me | Me | C7 | MeCN | MeIm | 0.15 | 11.6 | 0.66 |
| Me | Me | C7 | MeCN | MeIm | 0.15 | 15.4 | 0.44 |
| Me | Me | C7 | MeCN | MeIm | 0.15 | 20.4 | 0.24 |
| Me | H | C3NMeC3 | MeCN | | | −20 | 0.054 |
| Me | H | C3NMeC3 | MeCN | | | −15 | 0.0051 |
| Me | H | C3NMeC3 | MeCN | a | | −20 | 0.011 |
| Me | H | C3NMeC3 | MeCN | a | | −15 | 0.0017 |

*a* Solution contained 1 equiv of *p*-toluic acid.

**Table 12.** Enthalpy and Entropy Values for Dioxygen Binding by Selected Lacunar Cyclidene Complexes[b] of the Formula $[Co(R^2R^3Cn[16]cyclidene)B]^{2+}$ [a]

| $R^3$ | $R^2$ | $R^1$ | $\Delta H$[c] | $\Delta S$[d] |
|---|---|---|---|---|
| Me | H | C5 | −15.2(6) | −65(2) |
| Ph | H | C5 | −14.3(6) | −62(2) |
| Me | Me | C5[e] | −16.7(10) | −63(3) |
| Ph | Me | C5 | −16.3(6) | −67(3) |
| Me | H | C7 | −17.3(5) | −64(2) |
| Me | Me | C7[f] | −17.25 | −61.5 |
| Ph | Me | C7 | −18.0(9) | −65(3) |

*a* In MeCN with 1.5 M 1-methylimidazole unless otherwise specified. *b* Other values have been reported for related compounds: Busch, D. H. In *Oxygen Complexes and Oxygen Activation by Transition Metals*; Martell, A. E., Sawyer, D. T., Eds.; Plenum Press: New York, 1988.*c* In kcal mol; numbers in parentheses are standard deviations. *d* In eu; numbers in parentheses are standard deviations. *e* In $H_2O$ with 2.5 M 1-methylimidazole. *f* In MeCN with 0.15 M 1-methylimidazole, $R^2 = 0.991$.

constant. As pointed out earlier, the structural element that correlates best with the dioxygen affinity is the width of the cleft created by the rising unsaturated chelate rings. This cavity width is controlled by the polymethylene chain length, increasing smoothly as the chain length increases from trimethylene through octamethylene. Figure 5 shows that the rate at which the affinity increases is strongly attenuated in the vicinity of the maximum limit at octamethylene. Longer bridges[9b,10b] lead to a change in the points of departure of the bridge from the nitrogen atoms of the superstructure, and this structural change is accompanied by a switch to decreasing cavity width with further increases in chain length (over the range from nonamethylene through dodecamethylene). As with shorter chains, the dioxygen affinity again changes in accord with cavity width. Thus octamethylene
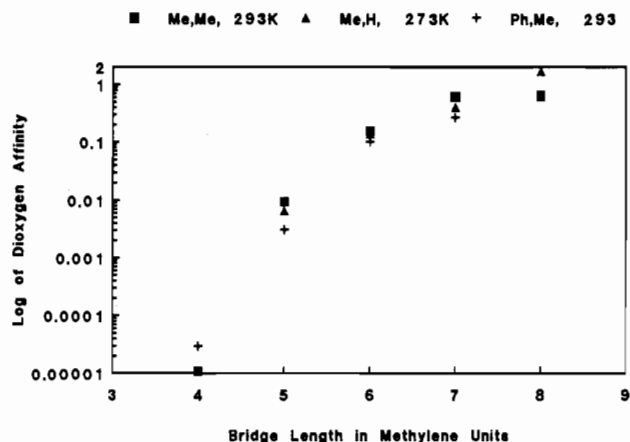


**Figure 5.** Variation of dioxygen affinity with the length of the bridge that spans the lacuna. The three sets of data differ, respectively, in the substituents $R^3$ and $R^2$.

represents a true maximum in both the cavity width and the dioxygen affinity for the cobalt complexes of [16]cyclidenes.

**Effects of Substituents $R^2$ and $R^3$ on Dioxygen Affinities.** The effects of $R^2$ and $R^3$ on dioxygen affinities of the cobalt(II) [16]-cyclidene complexes can be extracted from Table 10. Considering, first, cases in which $R^3 = $ Me, the dioxygen affinities of complexes with an electron-donating methyl group attached to the nitrogen atoms of the superstructure (the $R^2$ position) are always greater than those of complexes having hydrogen atoms at $R^2$, but the magnitude of this effect depends strongly on the length of the bridging $R^1$ polymethylene group. For the relatively short C5 bridge, the ratio of the equilibrium constants, $K_{O_2}$, for $R^2 = $ Me divided by $K_{O_2}$ for $R^2 = $ H, averages about 12, decreasing to 9
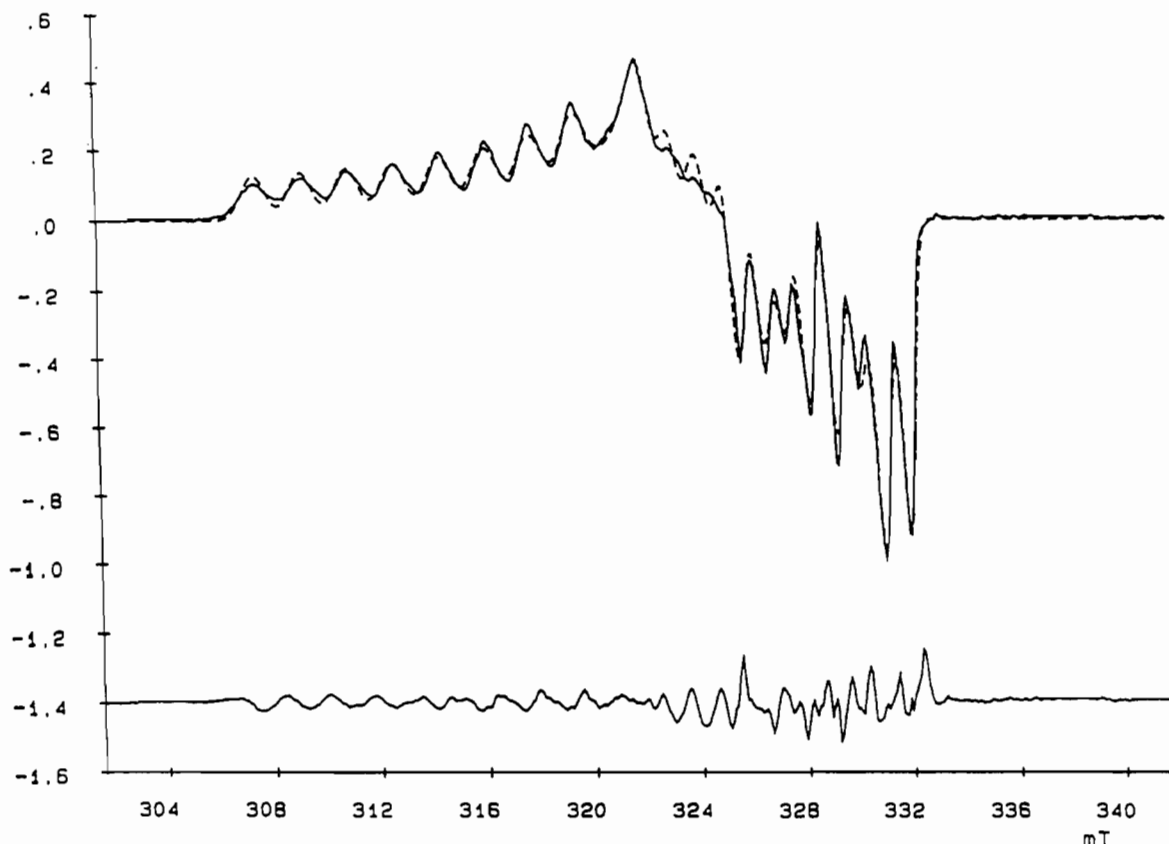
**Figure 6.** Observed and simulated ESR spectra for a typical cobalt lacunar [16]cyclidene dioxygen adduct: [Co(MeMeC6[16]cyclidene)(MeIm)-(O$_2$)]$^{2+}$ in acetone/1-methylimidazole at 77 K.

for C6, to 6 for C7, and finally to 3 for C8. When the same structural variations are considered for the examples where R$^3$ = Ph, the same general behavior is observed but the effect is diminished by a factor greater than 2. Further, the effects of PhCH$_2$ or PhCH$_2$CH$_2$ at the R$^2$ position are very similar to those of methyl groups.

In the R$^3$ position on the vinyl group of the cyclidene ring, replacing the vinyl hydrogen atom with a methyl group or placing a *t*-Bu in this position increases the dioxygen affinity dramatically. For example for the C6-bridged species having R$^2$ = Me, at –10 °C, $K_{O_2}$ = 0.026 for the complex with R$^3$ = H while $K_{O_2}$ = 4.6 for R$^3$ = Me, a ratio of approximately 180. In contrast, replacing a Me at the R$^3$ position with a Ph group shows less dramatic yet more complicated changes, increasing by a small factor when R$^2$ is methyl and showing a similar decrease when R$^2$ is hydrogen. Effects of *n*-Bu and *n*-Pr groups are similar, appearing to be some 50% larger than those of a methyl group.

The effects described above for the R$^2$ and R$^3$ substituents can be ascribed to the electron-donating abilities of the substituents. Because of the conjugated systems in the cyclidene ligands, the electron-donating abilities of the R$^2$ and R$^3$ groups have immediate effects on the electron density at the cobalt center, which in turn determines the dioxygen affinity of any given cyclidene complex. Earlier studies have shown that the electrode potentials of the Ni(III/II) couples of nickel cyclidene complexes reflect the electron-donating abilities of the ligand.[16,24] For example, both H and Ph are electron withdrawing when compared to methyl groups at the R$^3$ positions. This simple electronic argument accounts very well for most of the effects of the R$^2$ and R$^3$

substituents on the dioxygen affinities of the Co(II) [16]cyclidene complexes. However, the striking increase in sensitivity toward electron-donating groups as the bridging group is shortened, which is found for dioxygen affinities, is not mirrored in the electrochemical data. Since shorter bridges act sterically to diminish the dioxygen affinity, the enhanced sensitivity of the dioxygen affinity to electronic effects may be viewed in analogy to the *selectivity–reactivity principle*. When the dioxygen affinity is diminished sterically, the influence of electronic factors is enhanced; i.e., the less the reactivity (lower dioxygen affinity), the greater the selectivity (electronically).

A trend that cannot be so simply explained arises from the contrasting behavior of phenyl and methyl groups at the R$^3$ position when R$^2$ is hydrogen. For pentamethylene-bridged complexes, the dioxygen affinities show almost no change when phenyl and methyl are interchanged at the R$^3$ position, but an inverted effect is observed for the hexamethylene-bridged complexes. $K_{O_2}$ is some 2–3 times greater for the phenyl derivatives than for the methyl counterpart. While no adequate explanation is at hand, we suspect that the behavior may be associated with the substantial acidity of the proton R$^2$ (on nitrogen). Thus hyperconjugative effects might emphasize different resonance forms for the delocalized chelate rings in the phenyl and methyl derivatives.

In sharp contrast to the size of an R$^1$ group, which controls the dimension of the cavity and the dioxygen affinity, the sizes of R$^2$ and R$^3$ substituents are expected to have no substantial effects on dioxygen affinity, an assumption that is consistent with the preceding discussion. It is obvious that the size of R$^2$ will have little effect on $K_{O_2}$ since R$^2$ is far away from the cavity. Even though R$^3$ is located at the entrance of the cavity, it is likely that its steric effects are also small because the R$^3$ groups point outward and away, continuing the general tapering shape of the cavity. The hydrophobic character of bulkier groups at the R$^3$ site may effectively extend the cavity volume, providing additional shielding for the small ligand therein. Since dioxygen affinities are known

(24) The Co(III/II) couple is highly dependent on the bridging group R$^1$, which strongly affects the coordination number change that accompanies the redox process. See, for examples: (a) Saveant, E. V. *Electrochim. Acta* **1963**, *8*, 905. (b) Chavan, M. Y.; Meade, T. J.; Busch, D. H.; Kuwana, T. *Inorg. Chem.* **1986**, *25*, 314. (c) Chia, P. S. K.; Masarwa, M.; Warburton, P. R.; Wu, W.; Kojima, M.; Nosco, D.; Alcock, N. W.; Busch, D. H. *Inorg. Chem.* **1993**, *32*, 2736.

**Table 13.** ESR Parameters of Oxygenated Cobalt Cyclidene Complexes in Frozen Solutions in Acetone Containing Axial Base[a]

| $R^1$ | $R^2$ | $R^3$ | B | $g_x$ | $g_y$ | $g_z$ | $A_x$ | $A_y$ | $A_z$ | $\langle A \rangle$ | $\alpha \pm 0.3$ |
|---|---|---|---|---|---|---|---|---|---|---|---|
| Me | Me | Me | MeIm | 2.010 | 2.090 | 1.993 | 5.5 | 20.1 | 9.0 | 11.5 | 31.1 |
| Me | Me | Ph | MeIm | 2.010 | 2.091 | 1.993 | 6.4 | 18.8 | 8.6 | 11.3 | 29.2 |
| C4 | Me | Me | MeIm | 2.008 | 2.086 | 1.991 | 6.4 | 19.7 | 8.9 | 11.7 | 29.6 |
| C4 | Me | Me | py | 2.010 | 2.086 | 1.993 | 5.9 | 19.5 | 8.7 | 11.4 | 29.8 |
| C4 | Me | Ph | MeIm | 2.011 | 2.097 | 1.993 | 6.4 | 19.7 | 8.3 | 11.5 | 30.2 |
| C4 | H | Ph | MeIm | 2.012 | 2.096 | 1.993 | 6.1 | 20.0 | 8.4 | 11.5 | 30.0 |
| C5 | Me | Me | MeIm | 2.010 | 2.091 | 1.995 | 7.2 | 19.3 | 8.6 | 11.7 | 30.8 |
| C5 | Me | Me | py | 2.011 | 2.091 | 1.993 | 5.6 | 20.7 | 8.9 | 11.7 | 29.7 |
| C5 | Me | Ph | MeIm | 2.012 | 2.093 | 1.994 | 6.8 | 19.0 | 8.4 | 11.4 | 28.4 |
| C5 | H | Ph | MeIm | 2.011 | 2.091 | 1.993 | 6.2 | 19.8 | 8.6 | 11.5 | 29.0 |
| C6 | Me | Me | MeIm | 2.009 | 2.088 | 1.992 | 6.1 | 19.6 | 8.9 | 11.6 | 31.6 |
| C6 | Me | Me | py | 2.009 | 2.087 | 1.992 | 5.3 | 19.8 | 8.8 | 11.3 | 31.3 |
| C6 | Me | Ph | MeIm | 2.009 | 2.089 | 1.993 | 6.6 | 18.0 | 8.3 | 11.0 | 30.6 |
| C6 | H | Ph | MeIm | 2.009 | 2.087 | 1.993 | 6.9 | 18.1 | 8.4 | 11.1 | 29.5 |
| C7 | Me | Me | MeIm | 2.011 | 2.090 | 1.995 | 6.6 | 19.5 | 8.7 | 11.6 | 28.7 |
| C7 | Me | Me | py | 2.010 | 2.088 | 1.993 | 6.4 | 19.5 | 8.8 | 11.6 | 30.0 |
| C7 | Me | Ph | MeIm | 2.009 | 2.086 | 1.992 | 7.0 | 18.3 | 8.4 | 11.2 | 28.0 |
| C7 | H | Ph | MeIm | 2.009 | 2.087 | 1.993 | 6.6 | 18.7 | 8.6 | 11.3 | 28.7 |
| C8 | Me | Me | MeIm | 2.009 | 2.086 | 1.992 | 6.3 | 19.2 | 8.4 | 11.3 | 27.0 |
| C8 | Me | Me | py | 2.010 | 2.089 | 1.991 | 5.7 | 20.3 | 8.7 | 11.6 | 27.7 |
| C8 | Me | Ph | MeIm | 2.009 | 2.088 | 1.992 | 6.2 | 18.5 | 8.4 | 11.0 | 28.4 |
| C8 | H | Ph | MeIm | 2.009 | 2.088 | 1.992 | 7.1 | 18.4 | 8.4 | 11.3 | 27.8 |
| C9 | Me | Me | MeIm | 2.010 | 2.090 | 1.994 | 6.5 | 19.2 | 8.5 | 11.4 | 27.2 |
| C9 | Me | Me | py | 2.009 | 2.090 | 1.991 | 5.9 | 20.2 | 8.8 | 11.6 | 27.8 |
| C10 | Me | Me | MeIm | 2.011 | 2.090 | 1.994 | 6.6 | 19.1 | 8.4 | 11.4 | 27.7 |
| C10 | Me | Me | py | 2.010 | 2.090 | 1.991 | 6.0 | 20.0 | 8.7 | 11.6 | 29.5 |
| C11 | Me | Me | MeIm | 2.009 | 2.088 | 1.993 | 6.3 | 19.2 | 8.4 | 11.3 | 29.1 |
| C11 | Me | Me | py | 2.009 | 2.089 | 1.991 | 6.3 | 19.8 | 8.8 | 11.6 | 29.6 |
| C12 | Me | Me | MeIm | 2.011 | 2.091 | 1.995 | 6.3 | 19.3 | 8.4 | 11.3 | 28.8 |
| C12 | Me | Me | py | 2.009 | 2.090 | 1.991 | 5.9 | 20.4 | 8.6 | 11.6 | 30.2 |
| m-Xyl | Me | Me | MeIm | 2.010 | 2.089 | 1.992 | 5.6 | 19.4 | 8.1 | 11.0 | 32.5 |
| durene | pip | Me | MeIm | 2.009 | 2.086 | 1.993 | 5.4 | 19.3 | 8.6 | 11.1 | 30.3 |

[a] Values of $A$ are reported in cm$^{-1}$ ($\times 10^4$) and those of $\alpha$ in degrees.

to increase with solvent polarity, such a hydrophobic effect would be expected to act counter to the observations.

**Other Effects on Dioxygen Affinities.** Other steric effects are evident in the derivatives having pairs of methyl substituents on the central carbon atoms of their saturated chelate rings. These are identified in Tables 10 and 11 by the letters "DM" preceding or following [16], the latter being present to indicate the parent 16-membered cyclidene macrocycle. If DM precedes [16], then the *gem*-dimethyl groups are adjacent to the greater opening in the lacuna while [16]DM indicates that the *gem*-dimethyl groups are beneath the lesser opening into the lacuna; DM[16]DM indicates two pairs of such groups. The MeMeC5 complex having DM[16] shows a decrease in dioxygen affinity from 0.215 to 0.046 Torr$^{-1}$, while the corresponding C6 derivatives show essentially no steric effect due to this bulky group. In fact, the MeMeC6DM[16]DM derivative has the same dioxygen affinity as that of MeMeC6[16]. The confining cavity and lack of flexibility of the C5 bridge probably generate a steric conflict between the bound $O_2$ and the axial methyl of the *gem* pair that C6 does not cause because of the commodious nature of the larger cavity. Larger decreases in $O_2$ affinity attributable to *gem*-dimethyl groups have been found with the iron(II) cyclidenes having *m*-xylylene bridges.[6i] A single data point for the octamethylene-bridged complex suggests that the presence of the *gem*-dimethyl groups near the lesser opening to the cavity may increase the dioxygen affinity. Replacing the hydrogens on the center methylene group of the pentamethylene bridge by *gem*-dimethyl groups decreases the $O_2$ affinity by a factor of 2–6, and replacing the methylene group with an oxygen atom causes an increase in affinity of about the same magnitude. Both changes are believed to arise from steric effects.

The center methylene group of the heptamethylene bridge has been replaced by a methyl-substituted nitrogen atom in the expectation that hydrogen-bonding effects might be observed between the basic nitrogen and bound $HO_2$ or between its protonated derivative and bound $O_2^-$.[25] These structural alterations consistently decreased the dioxygen affinities of the cyclidene complexes rather than producing the anticipated enhancements, and the effect is large, approaching a factor of 100. This unexpected result is rationalized on the assumption that the primary interaction involving the amino group, or its protonated form, is with solvent rather than with the bound dioxygen. Consequently, the group stabilizes conformations that disfavor dioxygen binding.

The $K_{O_2}$ values in Table 11 show that the cobalt(II) complexes of [16]cyclidenes follow the general rules: the more polar the solvent and the stronger the axial base, the higher the $O_2$ affinity. For example, the $K_{O_2}$ values of [Co$^{II}$(MeMeC6)]$^{2+}$ in 2.5 M 1-methylimidazole at 10 °C are 4.5 Torr$^{-1}$ in $H_2O$ and 1.06 Torr$^{-1}$ in DMF. The $K_{O_2}$ values of [Co$^{II}$(MeMeC6)]$^{2+}$ in MeCN at –10 °C are 0.006 Torr$^{-1}$ with no other axial ligand, 0.19 Torr$^{-1}$ in 1 M pyridine (acetone solvent), and 4.6 Torr$^{-1}$ with 1.5 M 1-methylimidazole.

**ESR Spectroscopic Studies of the Dioxygen Adducts of Cobalt-(II) [16]Cyclidene Complexes.** ESR spectroscopy has proven especially useful for examining dioxygen binding to cobalt(II) complexes, since both the five-coordinate cobalt(II) complexes and the 1:1 cobalt–dioxygen adducts have distinctive ESR spectra, a relationship that has long been appreciated.[26] ESR spectroscopy has been used to examine the electronic nature of the cobalt–dioxygen bond,[1d,27] and the ESR properties of a large number of cobalt–dioxygen complexes have been collected in reviews.[1d,e] The ESR spectrum is dependent upon both the electronic and geometric properties of the molecule of interest. In recent years, more detailed information has been forthcoming from ESR spectroscopy through computer simulation of the spectra; and further details may be found in the review by Smith and Pilbrow.[1d]

(25) (a) Phillips, W. D. V.; Schoenborn, B. P. *Nature* **1981**, *292*, 81. (b) Gerothanassis, I. P.; Momenteau, M.; Loock, B. *J. Am. Chem. Soc.* **1989**, *111*, 7006.
(26) Diemente, D.; Hoffman, B. M.; Basolo, F. *J. Chem. Soc., Chem. Commun.* **1970**, 467.
(27) (a) Tovrog, B. S.; Kitko, D. J.; Drago, R. S. *J. Am. Chem. Soc.* **1976**, *98*, 5144. (b) Drago, R. S.; Corden, B. B. *Acc. Chem. Res.* **1980**, *13*, 353.
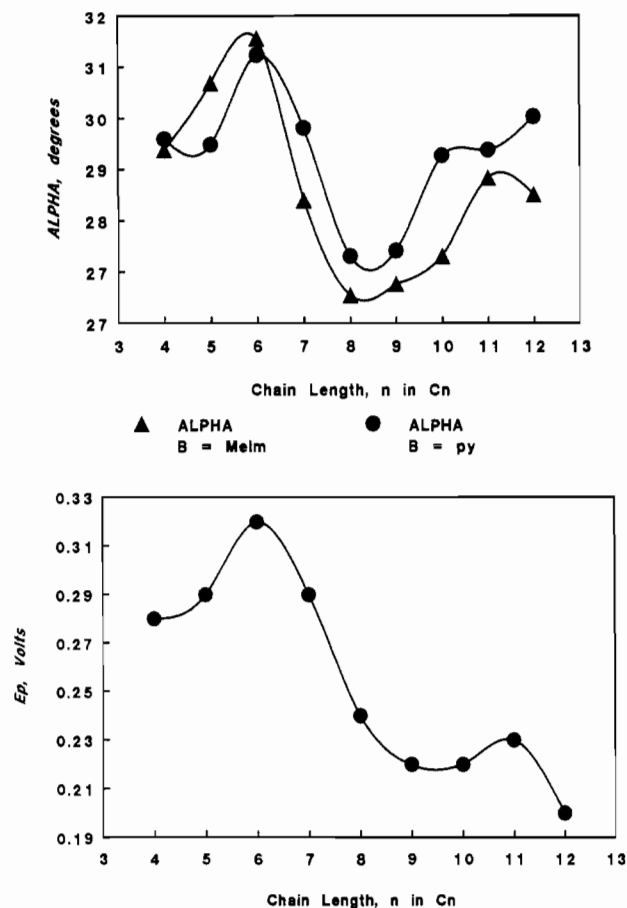
**Figure 7.** Variation of the estimated $CoO_2$ angle $\alpha$ with the length of the polymethylene bridge that spans the lacuna in cobalt cyclidene complexes and the parallel behavior of cyclovoltammetric peak potentials: (a, top) variation of $\alpha$ with bridge chain length; (b, bottom) variation with bridge length of CV peak potential for $[Co(MeMeCn[16]-cyclidene)]^{2+}$ in methylene chloride.

In this work, the ESR spectra for a series of cobalt(II) cyclidene complexes were interpreted using computer simulation. The spectra of the oxygenated cobalt cyclidene complexes in frozen acetone solutions all appear to be very similar, but good spectral resolution allows us to evaluate very fine differences in the intensities of the individual peaks. An illustration showing the observed and calculated ESR spectra is presented in Figure 6. It should be noted that deviations between observed and calculated spectra are relatively equally distributed over the whole range of magnetic fields.

The spin Hamiltonian parameters obtained by simulations for the dioxygen adducts of the cobalt(II) cyclidene complexes are presented in Table 13. The parameter $\alpha$ has received the most attention since it is easily visualized (the Co–O–O angle = $\alpha$ + 90°). The angle $\alpha$ is also amenable to independent measurement (in X-ray crystal structures) and thus provides a convenient parameter to judge the accuracy of the model employed in these calculations. The only available X-ray structure of an oxygenated cobalt cyclidene complex is that described above for $[Co(MeMeC6)(1-MeIm)(O_2)](PF_6)_2$. The Co–O–O bond angle was found to be 121 ± 1°, which is equivalent to a value of $\alpha = 31 \pm 1°$. This value is in very good agreement with the value of 31.6 ± 0.3° estimated for this complex on the basis of ESR simulation (Table 13). The dependence of $\alpha$ on the length of the polymethylene bridge ($R^1 = Cn$) is shown in Figure 7a for the series of cyclidene complexes with $R^2 = R^3 = Me$. It is apparent that the Co–O–O angle does not correlate with the dioxygen affinity, which, along with the cyclidene ligand cavity width, increases systematically from $n = 4$ to $n8$ and then decreases for $n = 9–12$.[10b] A correlation has been observed between the dependence of $\alpha$ on
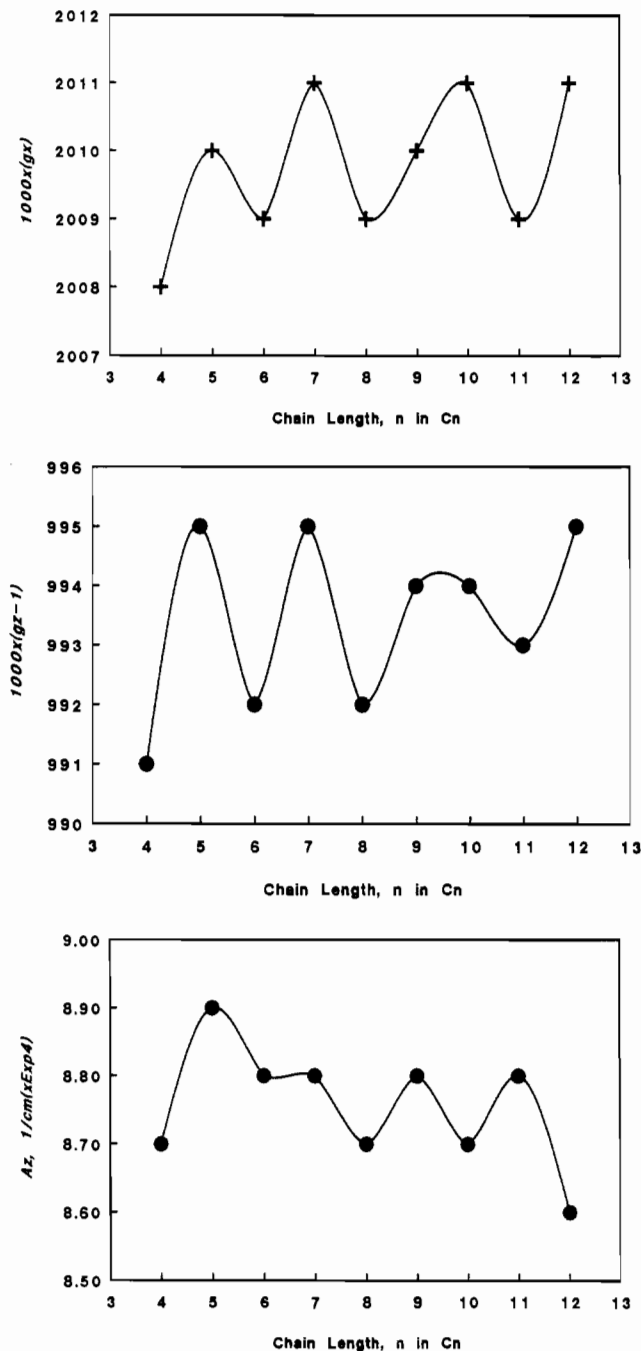


**Figure 8.** ESR spectra of $[Co(MeMeCn[16]cyclidene)B(O_2)]^{2+}$: (a, top) variation of $g_x$ with chain length $Cn$, B = MeIm; (b, middle) variation of $g_z$ with chain length $Cn$, B = MeIm; (c, bottom) variation of $A_z$ with chain length $Cn$, B = py.

cyclidene bridge length and the cobalt(III/II) redox potential obtained from cyclic voltammetry in noncoordinating media (Figure 7b). Methylene chloride was used as the solvent since the cyclic voltammograms of cobalt(II) cyclidene complexes in coordinating solvents of small steric bulk are known to become increasingly irreversible as the ligand cavity size increases, presumably because the solvent molecule can coordinate within the cavity of the cobalt(III) derivative.[24] The correlation of $\alpha$ with the cobalt(III/II) redox potential presumably indicates that the Co–O–O angle depends upon the electron density at the metal center. The underlying cause of the change in the redox potential with bridge length remains uncertain; however, it is not a simple function of overlap between the ligand orbitals and the metal d orbitals. This overlap would be expected to depend upon the angle of the unsaturated portion of the cyclidene ligand to the $N_4$ plane, which in turn will depend on the cavity width, and no

such correlation exists. Also, the $\alpha$ value for C6 is the largest, with that of C5 a close second. These two complexes have cavity widths ($C_4$–$C_4'$ distances: 6.55 and 6.63 Å, respectively)[9c] most similar to that of the unbridged complex ($C_4$–$C_4'$ distance: 6.50 Å)[9d] and presumably are the least strained complexes in the series. However, the relationship between the strain of a dioxygen carrier and the $\alpha$ angle of its dioxygen adduct is not well understood.

The influence of the axial donor on the ESR parameters has been examined for the series $[Co(MeMeCn)B(O_2)]^{2+}$, where the axial base B = pyridine (py) or 1-methylimidazole (MeIm), but no great regularity has been found. The Co–O–O angle is smaller for pyridine than for 1-methylimidazole, with the exception of $Cn$ = C5 and C6. Similar trends are observed for the spin Hamiltonian parameters: $A_x$(MeIm) > $A_x$(py) except for $Cn$ = C12; $A_z$(py) > $A_z$(MeIm) above $n$ = 7; $g_z$(MeIm) > $g_z$(py) except for $n$ = 4; $A_y$(py) > $A_y$(MeIm) except for $n$ = 4 and 7.

Changes in the $R^2$ and $R^3$ substituents on the macrocyclic ligand also have an impact on the hyperfine parameters. Replacement of the $R^3$ methyl groups by phenyl substituents typically results in lower values of $A_y$ and $A_x$. The effect on the ESR parameters presumably is derived from the electron-withdrawing properties of the phenyl groups which also reduce the dioxygen affinity of the cobalt(II) complexes (vide supra) and shift the metal redox potential to more positive values.

In the series where $R^2$ = $R^3$ = Me, neither the Zeeman nor the hyperfine parameters change in a systematic manner with the number of polymethylene units in $R^1$. In contrast, the series with $R^3$ = Ph shows a systematic dependence of $A_y$ on the length of the polymethylene bridge. Thus, with $R^2$ = Me or H, the maximum values of $A_y$ were observed when $n$ = 4, and minimum values were obtained with $n$ = 6. Interestingly, in both groups values of $g_y$ vary in a similar manner, being highest for the shortest bridge. These differences may be interpreted as originating from changes in the electron-withdrawing capabilities of the $\pi$-system of the unsaturated portions of the ligand, extended by the phenyl

rings in the $R^3$ position. When the bridge is short, the dihedral angles between the Co–$N_4$ plane and the planes established by the unsaturated portions of the ligand are smaller than those with longer bridges or with no bridge at all. Larger dihedral angles indicate that the macrocycle has adopted a more nearly planar conformation,[9b] which is expected to favor delocalization of the electron density from the cobalt, thereby affecting $g_y$ and $A_y$ values. The similarity of the parameters for $[Co(PhMeC8)(1-MeIm)(O_2)]^{2+}$ and for the unbridged complex $[Co(MeMeMe)-(B)(O_2)]^{2+}$, for which the macrocyclic structure should be most relaxed, is consistent with this hypothesis.

The parameters $A_z$, $g_x$, and $g_z$ all show an alternating pattern as $Cn$ is increased. For $g_x$ and $g_z$, even-membered bridging groups give lower values than their odd-numbered neighbors for bridge lengths from C4 through C8, but the pattern inverts between C9 and C10 (Figure 8). Similar alternation effects have been observed for infrared O–O stretching frequencies of cobalt–dioxygen adducts[22] and for the $^{13}C$ NMR spectra of the carbons adjacent to, or part of, the unsaturated portions of the ligand of the nickel(II) cyclidene complexes.[9b,28] These alternations are believed to arise from differences in the strain of the $R^1$ bridge due to the dissymmetry of the middle two carbon atoms in the even-membered polymethylene bridges.

**Supplementary Material Available:** Listings of isotropic and anisotropic thermal parameters, full bond lengths and angles, and hydrogen atom coordinates (6 pages). Ordering information is given on any current masthead page.

(28) Goldsby, K. A.; Meade, T. J.; Kojima, M.; Busch, D. H. *Inorg. Chem.* **1985**, *24*, 2588.